PANA-NOAA-CAL1

Report on the

Proton Calibration of HEPADs SN6 and SN9

at the

Alternating Gradient Synchrotron

of

Brookhaven National Laboratory

PANAMETRICS, INC.
221 Crescent Street
Waltham, Massachusetts 02254

August 5, 1986

Prepared for

NOAA/ERL/SEL
325 Broadway
Boulder, Colorado 80303

Under Contract No. NA84RAC05108

TABLE OF CONTENTS

LIST OF ILLUSTRATIONS

LIST OF TABLES

LIST OF TABLES (cont'd)

1.0 INTRODUCTION

Two HEPADs, SN6 and SN9, have been calibrated in detail at the Brookhaven National Laboratory Alternating Gradient Synchrotron (BNL AGS). A time-of-flight (TOF) system supplied by the Aerospace Corporation was used to select narrow energy width proton beams from a broader magnet-selected proton beam. The TOF system was implemented to eliminate spurious secondary proton energy responses and provided good proton selection for HEPAD calibration.

The HEPAD responses were measured as outlined in the Calibration Plan of Ref. 1. The angular response measurements at high energy show that the 12° HEPAD response is a good approximation of the omnidirectional response, as found for lower energies in Ref. 2. A detailed calibration of both HEPADs was made at 12°, using both the proton channel (P1 to P4) outputs and the PMT DY10 pulse height spectra. Good agreement now exists between the present HEPAD 12° calibration and the lower energy calibration points of Ref. 2. The earlier BNL calibration data for HEPADs (Refs. 3,4) are modified because those data were contaminated by higher energy protons (see the discussion in Section 2.1). The 12° response to the BNL AGS relativistic peak is equal to the atmospheric muon zenith view response to within 5%. The lower energy proton channels P1 and P2 have a response to rear entry high energy protons. The rear entry response to the relativistic peak measured at BNL is in agreement with the nadir view atmospheric muon response.

The analyzed data provide a final calibration curve with $\pm 1\sigma$ energy spread curves, shown in Fig. 3.5. The level sensor (LS) values and the PMT gain data for the HEPAD alpha lamps are given in Section 3.5. These data allow the in-orbit PMT gain adjustment and measurement for each HEPAD, and the determination of the resulting energy ranges for P1 to P4 and A1, A2. The calibration data presented in this report should apply to any HEPAD with the same detector geometry and shielding, and with similar electronics for pulse processing.

The details of the BNL AGS experimental configuration are presented in Section 2.1, while the data obtained are listed in Section 2.2. The detailed analysis of the data and the results are presented in Sections 3.1 to 3.5. Section 4.0 contains a short summary and conclusions.

2.0 EXPERIMENTAL CONFIGURATION AND LIST OF DATA OBTAINED

2.1 Experimental Configuration

The March 1985 HEPAD calibration at the BNL AGS used the A2 beam in the East Experimental Area. The experimental configuration was mostly as described in Ref. 1, with the basic set-up as shown in Fig. 2.1. A time-of-flight (TOF) system using two thin plastic scintillators is used to select protons in an energy range much narrower than that provided by the quadrupole/dipole/quadrupole magnet system. The TOF scintillators were about two inches in diameter and were centered on the proton beam line using reference marks on the A2 beam area floor. The HEPAD was centered on the TOF scintillator area with the rotation axis centered between the two solid state detectors (see the HEPAD detector configuration in Fig. 2.2).

The monitor detectors consisted of a 750 micron thick 2 cm^2 fixed detector and a 1500 micron thick 0.25 cm^2 linear scanning detector (effective area was closer to 0.5 cm^2). The monitor detector electronics configuration is shown in Fig. 2.3. For normal runs only the 1500 micron detector was in the beam area defined by the TOF scintillators. The monitor detectors were used to scan the proton beam horizontally at 9 GeV/c to verify that the HEPAD was located in a uniform portion of the beam area. The scan results, plotted as the ratio of 1500 micron detector counts divided by the 750 micron detector counts, are shown in Fig. 2.4. The 9 GeV/c beam profile shows that the TOF rear scintillator/HEPAD center is about 2 cm offset from the beam center. However, the HEPAD width at 0^o has a beam variation of $\pm$ 2.5% maximum, and since all HEPAD data are gated by a HEPAD solid state detector coincidence (S5) which has a maximum width at 0^o, the offset does not affect the HEPAD data. Since the TOF/HEPAD alignment was determined by reference marks on the beam line floor, that alignment was easiest to recheck and so was maintained for all HEPAD calibration runs.

Initial testing of the TOF system was done with the background beam of relativistic muons. This beam should produce a single peak for particles whose v/c = 0.995, but two additional weaker peaks were observed on each side of the primary peak. After much testing it was concluded that these secondary peaks were from particles striking the first dynode of one of the TOF PMTs. The TOF PMTs are high gain, fast response tubes, needed to reduce the time width of the TOF system response. Particles striking the first dynode produce pulses large enough to trigger the fast threshold, but without the time delay of the electron passage from the photocathode to the first dynode. This effect was verified by centering the 1500 micron monitor detector on the rear TOF scintillator and taking a TOF spectrum in coincidence with the 1500 micron detector threshold output. This eliminated the shorter TOF secondary peak, as expected.

Any particle striking the first dynode of the rear (stop) TOF PMT is more than one inch away from the TOF scintillator - defined beam, and so is incapable of striking the sensitive area of the HEPAD. This is not true of the front (start) TOF PMT,

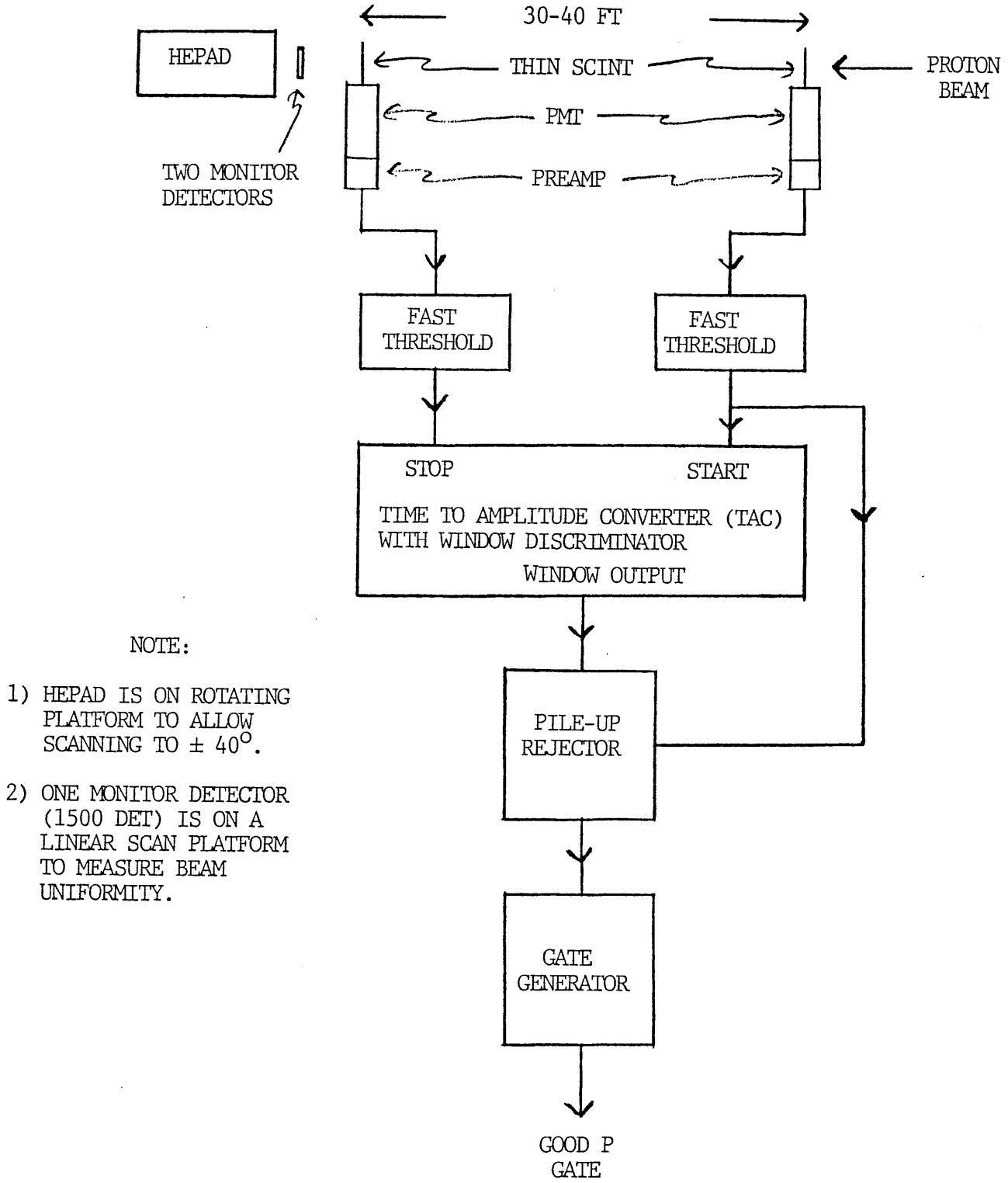

NOTE:

1) HEPAD IS ON ROTATING PLATFORM TO ALLOW SCANNING TO ± 40°.

2) ONE MONITOR DETECTOR (1500 DET) IS ON A LINEAR SCAN PLATFORM TO MEASURE BEAM UNIFORMITY.

Figure 2.1 Basic Set-Up for the BNL AGS HEPAD Calibration.

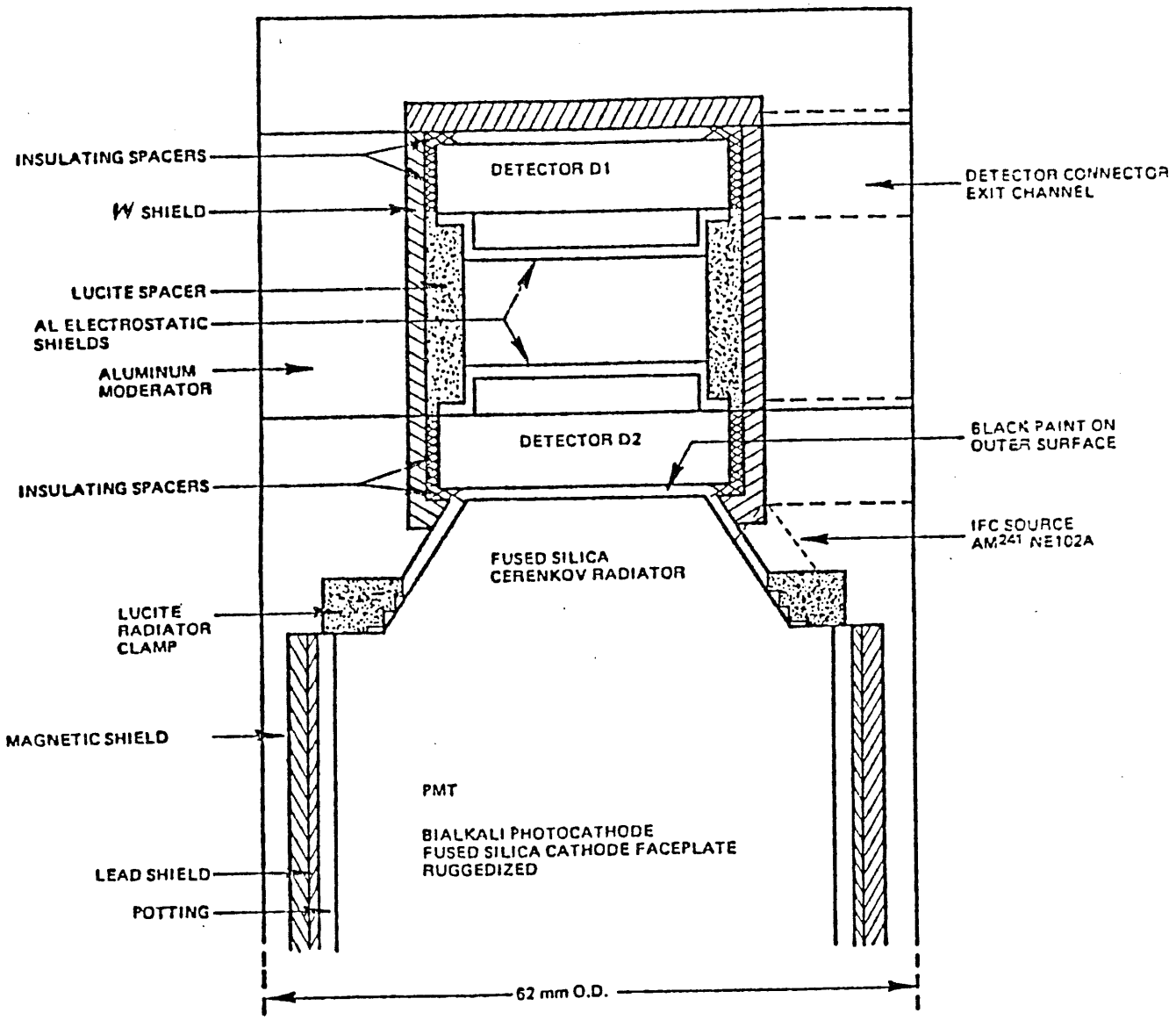

DETECTOR AREA: 3 cm^2
DETECTOR SEPARATION: 2.92 cm
GEOMETRIC FACTOR: G ≈ 0.9 cm^2-STER
ACCEPTANCE APERTURE: 68% OF G WITHIN < 24° HALF-ANGLE
100% OF G WITHIN < 34° HALF-ANGLE

Figure 2.2 HEPAD Telescope Subassembly - Detector End.

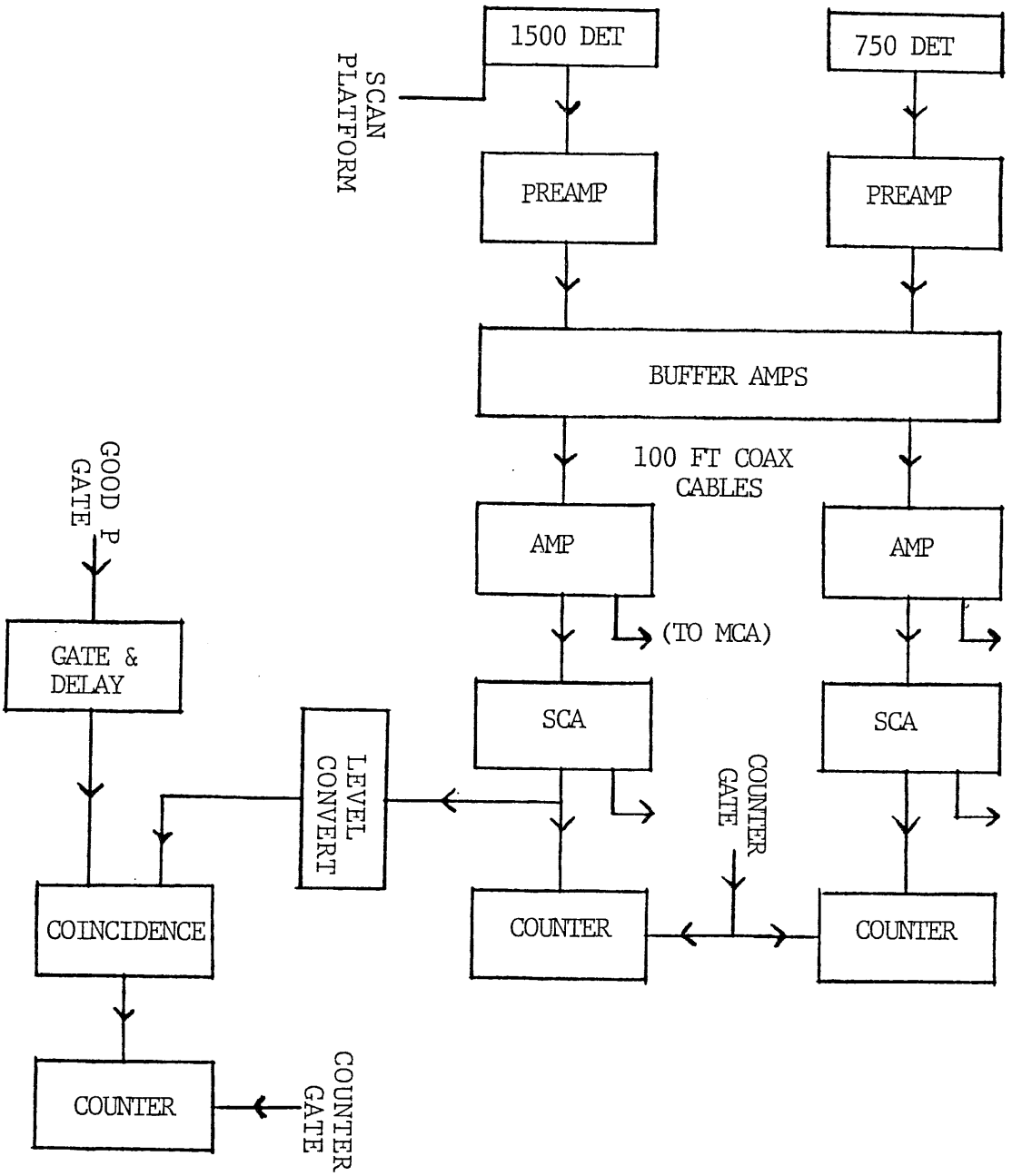

Figure 2.3. Details of the Electronics for the 750 Micron and 1500 Micron (Linear Scanning) Monitor Detectors.

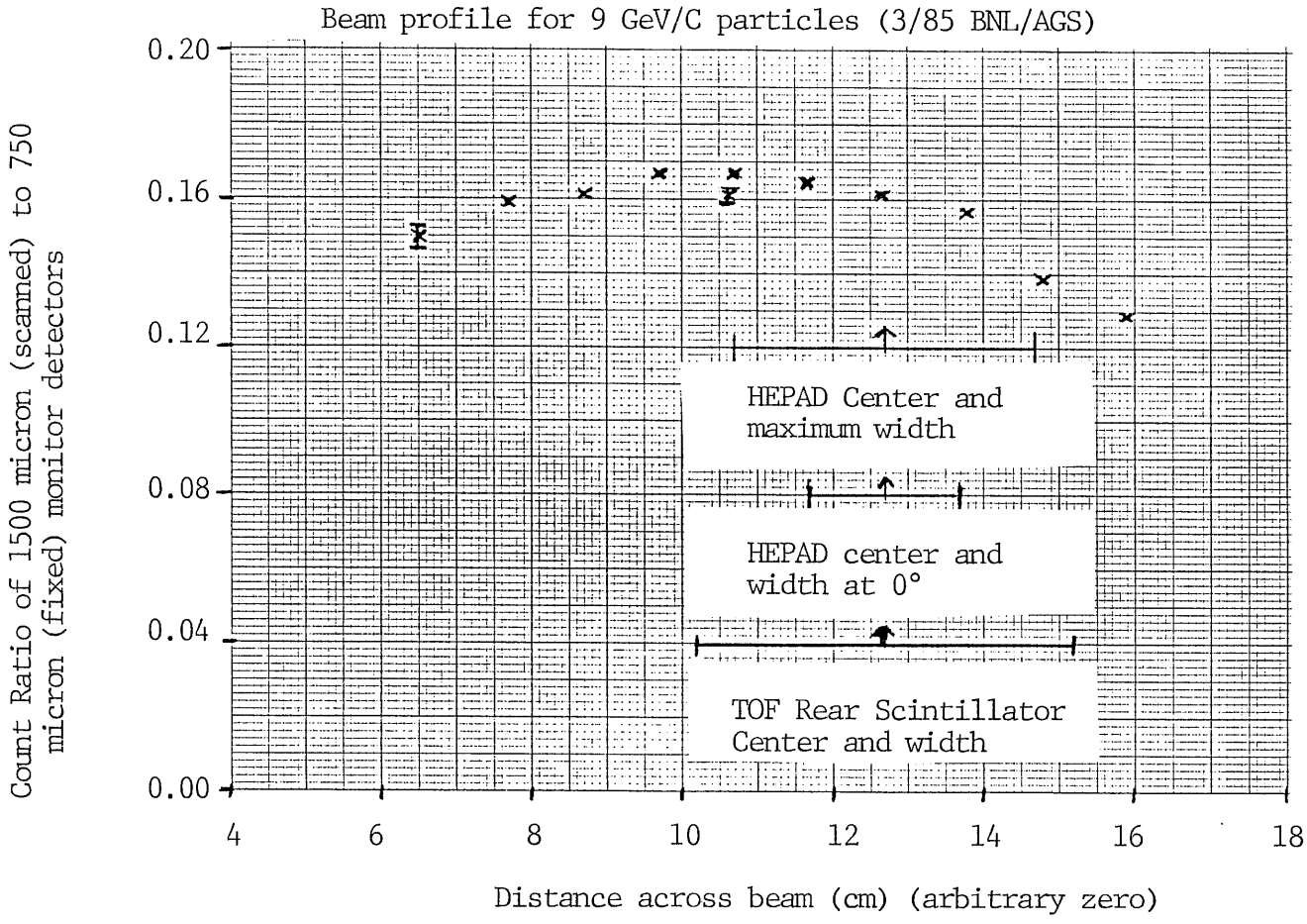

Figure 2.4. Horizontal Beam Profile at 9 GeV/C Measured with the Monitor Detectors.

where the TOF of a particle producing a first dynode pulse would appear earlier and so allow a higher energy particle to be gated (and counted) as a lower energy particle. This possibility was eliminated by using a second thin scintillator next to the start TOF scintillator, with the second PMT oriented away from the first PMT. The start TOF pulse was accepted as valid only if both PMTs produced pulses in coincidence, which occur only for particles passing through the overlap area of the two start scintillators. This eliminated the longer TOF secondary peak and the contamination of HEPAD data by higher energy particles. It should be noted that earlier HEPAD calibration data (Refs. 3, 4) may have some contamination from this effect.

The HEPAD electronics set-up is shown in Fig. 2.5. The external S5 pulse, a coincidence between the two HEPAD solid state detectors, was used with the Good P Gate (Fig. 2.1) to provide a Good P/External S5 Gate pulse for the HEPAD PMT spectra (DY10). The direct HEPAD particle outputs were all counted in coincidence with the Good P Gate as shown in Fig. 2.6. MCA spectra of various pulses, free or in coincidence with some logic pulse, were taken with the set-up shown in Fig. 2 7. This set-up was used to measure various threshold levels, with most of the data being taken for the DY10 spectrum in coincidence with the Good P Gate/Ext S5 pulse.

Particle counting was gated by a timer usually set to 100 or 200 seconds. In addition to the gated counts shown in Fig. 2.6 and the counts in Fig. 2.5 (gated and ungated), counters were also used to accumulate: Good P Gates; All S1 (no Good P Gate); Inhibits (from Pile-up rejector - Fig. 2.1); All TAC start scintillator pulses ; All TAC stop scintillator pulses. The auxiliary data allowed dead time and pile-up effects to be verified as being low.

2.2 HEPAD Data Obtained

HEPADs SN6 and SN9 were calibrated extensively with proton beams at the BNL AGS, and with atmospheric muon runs at Panametrics' Waltham facility (PI). The bulk of the proton calibration data is for a 12° incidence angle, which is a good approximation of the omnidirectional response (Ref. 2). HEPAD SN6 was determined to operate closest to the desired proton energy channels with PMT HV42, and a list of the 12° responses measured is given in Table 2.1. All of the listed energies had HEPAD output counts measured, while 9 out of 17 had PMT DY10 spectra measured.

Proton data at 12° obtained with HEPAD SN9 are listed in Table 2.2. Atmospheric muon data at PI originally gave HV36 as the best PMT operating voltage, but the 12° BNL proton data gave HV34 as the best level. Thus, data for a number of different HV steps were obtained. Count data in parentheses (yes) are not of direct value because they were obtained at a HV step different from the operating level.

The HEPAD angular response to higher energy protons was measured with SN6. Three energies were used, including the

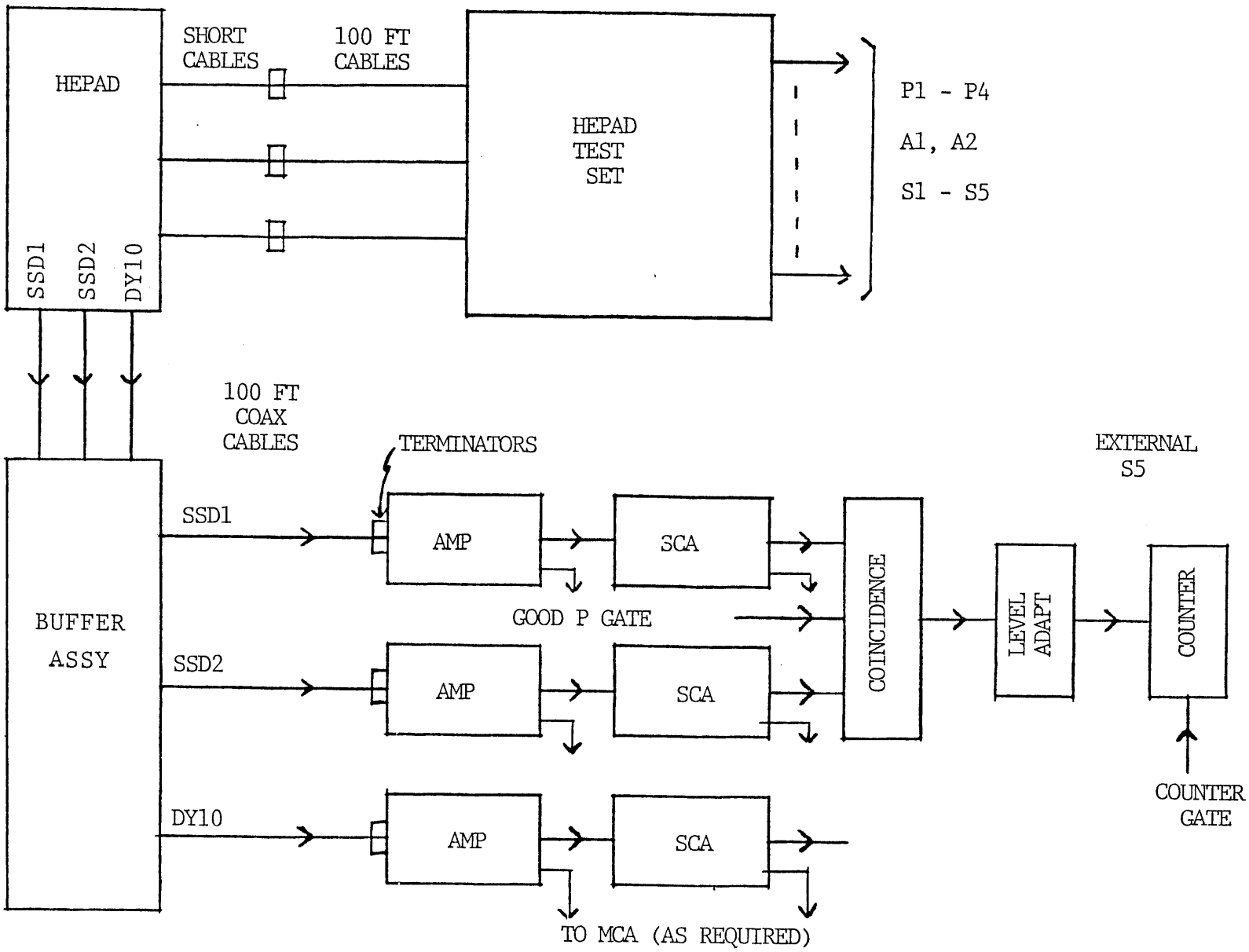

Figure 2.5 HEPAD Electronics Set-Up at the BNL AGS.

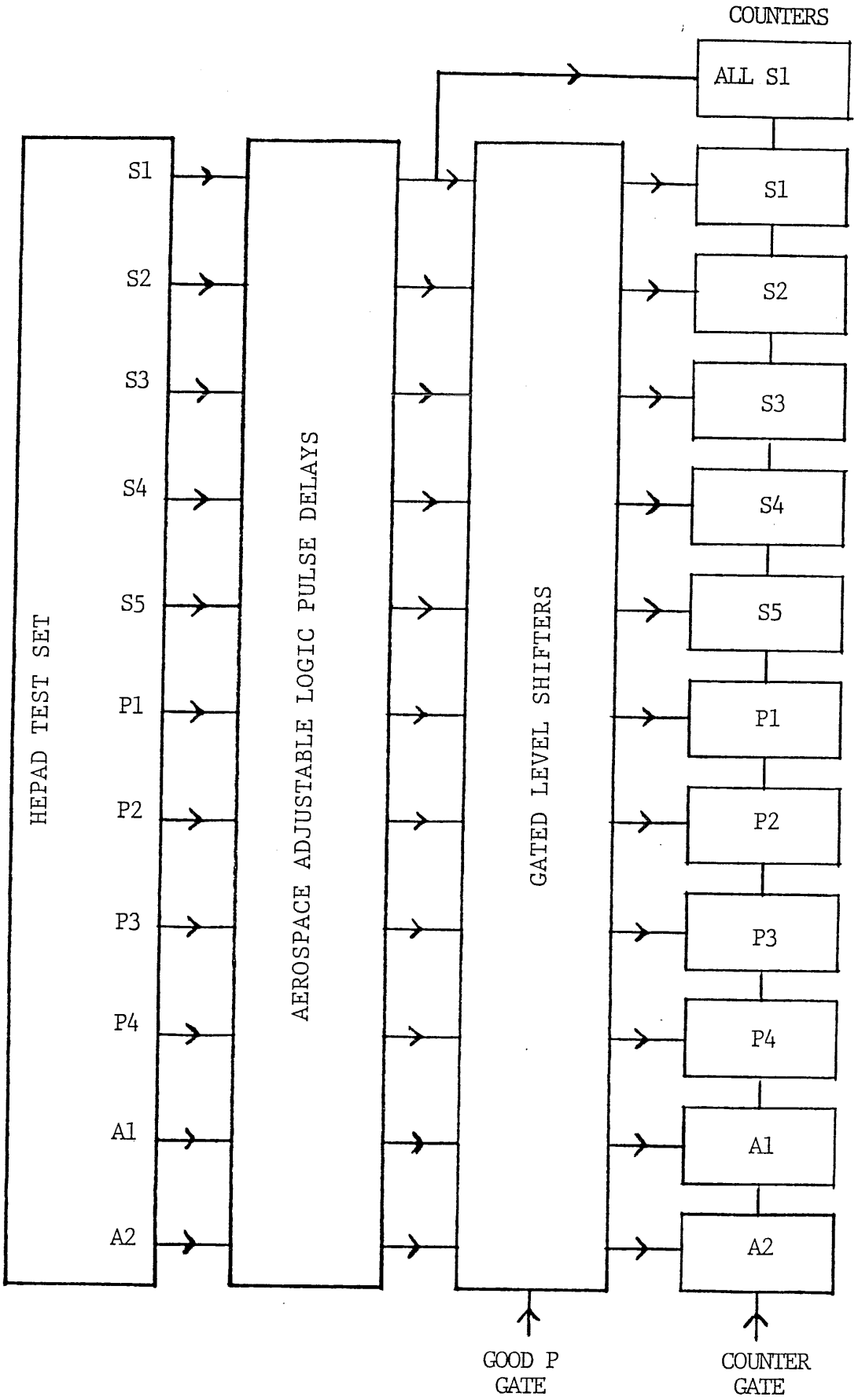

Figure 2.6 Electronic Set-Up for Counting the HEPAD Outputs.

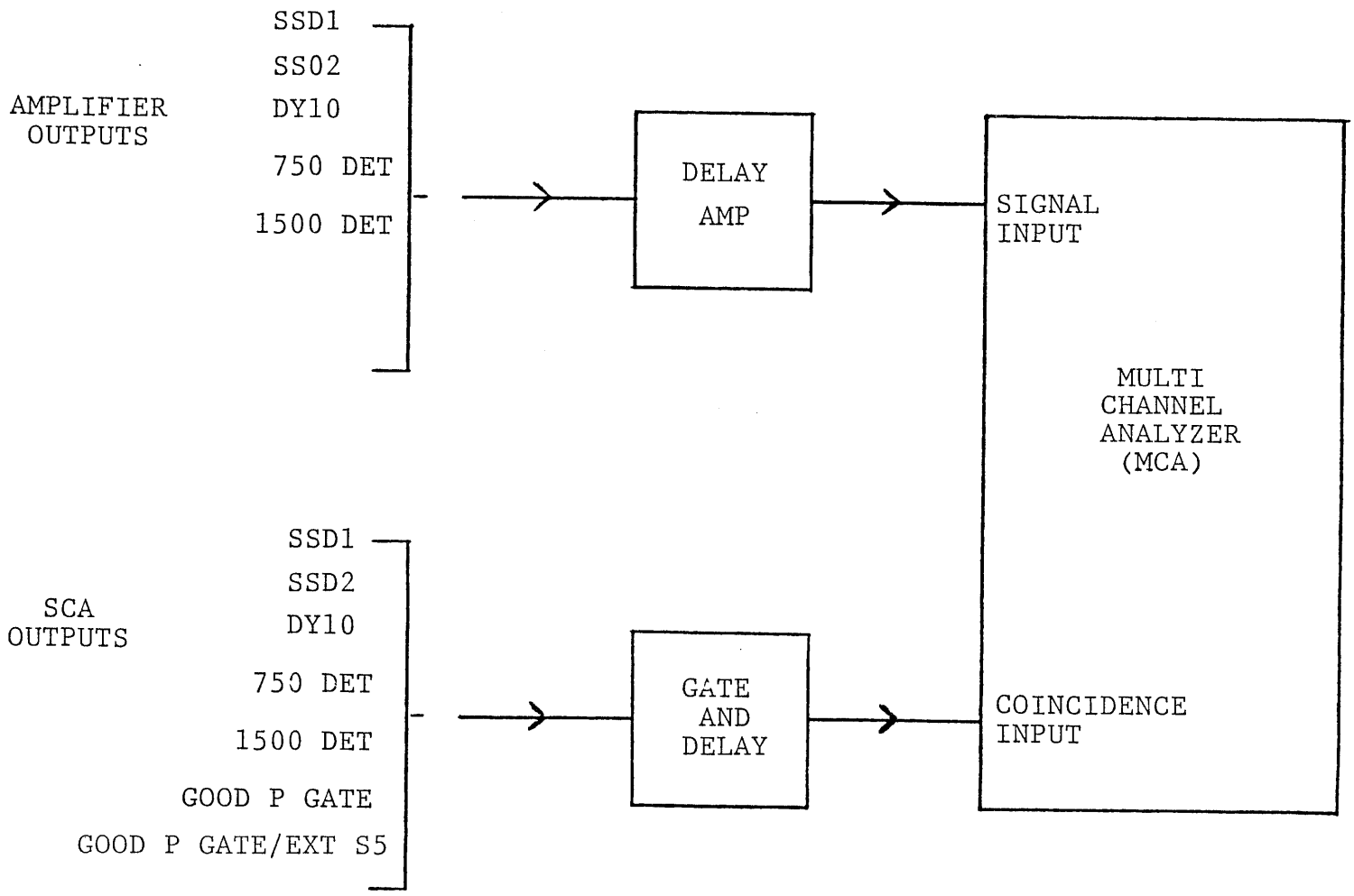

Figure 2.7 Electronics Set-Up for Measuring Pulse Height Spectra.

Table 2.1

March 1985 BNL AGS 12 Degree
Proton Data Obtained with HEPAD SN6 at HV42

Proton Energy (MeV)	Energy Width (MeV)	HEPAD Output Counts	HEPAD PMT DY10 Spectrum
Rel.Peak	--	yes	yes
1160	93	yes	--
1024	72	yes	--
883	74	yes	--
760	50	yes	--
695	43	yes	yes
626	35	yes	--
560	29	yes	yes
540	27	yes	yes
495	31	yes	--
460	43	yes	yes
438	39	yes	yes
407	53	yes	yes
397	69	yes	--
362	36	yes	yes
336	52	yes	--
307	28	yes	yes (x2 gain)

Table 2.2

March 1985 BNL AGS 12 Degree
Proton Data Obtained with HEPAD SN9

Proton Energy (MeV)	Energy Width (MeV)	HEPAD PMT HV levels	HEPAD Output Counts	HEPAD PMT DY10 Spectrum
Rel.Peak	--	36/33	(yes)	(yes)
932	76	34	yes	yes
807	61	34	yes	yes
772	57	36	(yes)	--
764	56	33/35/34	yes	yes
693	46	34	yes	yes
629	38	34	yes	yes
582	29	34	yes	yes
542	27	34	yes	yes
494	32	34	yes	yes
442	25	34	yes	yes
400	41	34	yes	yes
370	34	34	yes	yes (x2 gain)
343	33	34	yes	yes (x2 gain)
315	28	34	yes	yes (x2 gain)

relativistic peak. Both front and rear entry irradiations were made, the data obtained being listed in Table 2.3.

Atmospheric muon runs were made at PI for both HEPADs, both before and after the BNL AGS data were taken on March 18-21, 1985. The SN6 muon runs are listed in Table 2.4, and include a set from July 1984, when SN6 was delivered to Panametrics for integration with the GOES-G EPS. All the HEPAD SN6 data were taken at HV42.

The HEPAD SN9 atmospheric muon runs taken at PI are listed in Table 2.5. All muon runs, from initial runs prior to delivery from NOAA in December 1984, to the final muon runs prior to delivery to Hughes Aircraft Company for GOES-H in July 1985, are listed. The comments between muon run sets show the evolution and repair of a defective capacitor in the HEPAD. This capacitor affected the +6V current, and because of circuit designs it also affected the fast coincidence logic and some of the threshold values. The first indication of the problem occurred at BNL, when the IFC check showed a significant increase in the S5-on level, which also affected the P1-on level. The A1-on level was also significantly changed. The particle data at BNL did not seem to be affected.

HEPAD SN9 was returned to NOAA in April 1984, where the IFC checked out properly. Subsequently, it was found that the fast timing circuitry was coupled to the $\pm$ 6V supply voltages, and that these voltages were slightly different in the HEPAD BCUs at NOAA and at PI. The $\pm$6V supplies were adjusted to the EPS values, and the IFC now checked out properly at PI. At this point the $\pm$6V current increase became significant, while the upward trend worsened and the current became unsteady. Finally, in June 1985 the defective capacitor was diagnosed, and the HEPAD was repaired by NOAA. A final set of atmospheric muon runs was made at PI in July 1985. These muon runs gave a final operational check of the HEPAD, and the alpha lamp position was adjusted to the proper pulse height for LS2 (S4) at the desired PMT HV step of 34.

The difficulties with HEPAD SN9, which started about the time of the BNL AGS work, make the SN9 proton calibration data secondary to the SN6 data. The main HEPAD calibration results are based on the SN6 data, the SN9 data being used as partial verification. The results of the proton calibration are discussed in the following Sections.

Table 2.3

March 1985 BNL AGS Proton Angular Response
Data Obtained with HEPAD SN6 at HV42

Proton Energy (MeV)	Energy Width (MeV)	Front or Rear Incidence	Angles for which response was measured (counts and PMT DY10 spectra)
Rel. Peak	--	Front	0°, 12°, 24°, 36°
912	140	Front	0°, 12°, 24°, 36°
601	32	Front	0°, 12°, 24°, 36°
Rel. Peak	--	Rear	180°, 168°, 156°, 144°
900	141	Rear	180°, 168°, 156°, 144°
600	35	Rear	180°, 168°, 156°, 144°
269	28	Rear	180°

Table 2.4

Atmospheric Muon Data Taken With
HEPAD SN6 at HV42

Date Range	Type of Data Runs	Coincidence Requirements for PMT DY10 Spectra
7/16-20/84	Zenith Muon	S5; P4; P3; P2; P1
	Alpha Lamp	Free; S3; S4
	Alpha Lamp	S4/S3 ratio vs. HV step
3/11-14/85	Zenith Muon	S5; P4; P3
	Alpha Lamp	Free; S3; S4
3/25-26/85	Zenith Muon	S5
	Alpha Lamp	Free; S3; S4
	Alpha Lamp	S4/S3 ratio vs. HV step

Table 2.5

Atmospheric Muon Data Taken With HEPAD SN9

Date Range	PMT HV	Type of Data Runs	Coincidence Requirements for PMT DY10 Spectra
12/17-27/84	36	Zenith Muon	S5; P4; P3
	36	Nadir Muon	S5; P1; P2; P4
	36	Alpha Lamp	Free; S3; S4
	(+6V current increases from 34 mA to 35 mA)		
12/28/84-1/17/85	36	Zenith Muon	S5; P4; A1
	36	Alpha Lamp	Free
	0-50	Alpha Lamp	S4/S3 ratio vs. HV step
	(+6V current increases to 37 mA)		
3/26/85-4/1/85	34	Zenith Muon	S5; Ext S5; P4; P3
	34	Alpha Lamp	Free; S3; S4
	(Adjust ±6V levels on HEPAD BCU)/(+6V current reaches 40 mA)		
5/1-6/85	34	Zenith Muon	S5; P4; P3
	34	Alpha Lamp	Free; S3; S4
	(+6V current exceeds 40 mA and shows variations)		
5/17-20/85	34	Zenith Muon	S5; P4
	34	Alpha Lamp	Free; S3; S4
	(+6V current varies significantly, and at times exceeds 42 mA)		
6/3-5/85	34	Zenith Muon	S5; P4
	34	Alpha Lamp	Free; S3; S4
	(Defective capacitor replaced by NOAA)/(Final Alpha Lamp adjustment at PI)		
7/12-23/85	34	Zenith Muon	S5; P4; P3
	34	Nadir Muon	S5
	34	Alpha Lamp	Free; S3; S4
	20-50	Alpha Lamp	S4/S3 ratio vs. HV step

3.0 ANALYSIS OF DATA AND PRESENTATION OF RESULTS

3.1 HEPAD Angular Response for Protons

The HEPAD PMT angular response for protons of 561, 474, 412 and 368 MeV was reported in Ref. 2, and was used to justify the 12° response as an approximation of the response to an omnidirectional proton beam. As shown in Table 2.3, the angular response of HEPAD SN6 was measured for the relativistic peak, and for 912 and 601 MeV protons. The results from the SN6 data and from Ref. 2 are summarized in Table 3.1. The listed results for 24° and for the Ref. 2 data are averages of the 21° and 27° data. All results are normalized to the 12° peak for the energy in question, and give both the peak and the full-width-at-half-maximum (FWHM). For the 1985 BNL data, the average channel and FWHM based on the standard deviation (= 2.36 σ) are also given. The deviation of the peak from the average gives a measure of the asymmetry in the spectral shape.

The weighted average (Wtd Avg) spectra were calculated from the 0°, 12° and 24° spectra with weights of 0.104, 0.518, and 0.359 as calculated for two 3 cm^2 detectors separated by 2.92 cm. The component spectra were also normalized to a fixed total proton count to eliminate proton beam intensity variations. From Table 3.1 it can be seen that the relativistic peak has a significant asymmetry, with the average pulse height being about 5% higher than the peak. This asymmetry is less for 912 MeV and insignificant for 601 MeV.

The weighted average spectra equal the 12° spectra to within 10%, with most of the data being within $\pm$6%. The +10% deviation at 368 MeV is a small pulse height compared to the relativistic peak (only 1%) because of the low Cerenkov light output for 368 MeV protons (just above the Cerenkov threshold in quartz). The -9% deviation at 912 MeV is 7% compared to the relativistic peak, and may be partly due to increased errors in the weighted average spectra. The 601 MeV weighted average spectrum has the peak higher than the average pulse height, in contrast to the component spectra, which all have the peak equal to or below the average. It is felt that the 12° HEPAD response can be used to estimate the omnidirectional response to 5% of the relativistic proton response.

The angular response of the HEPAD changes character at about 600 MeV. Below 600 MeV the PMT response is near minimum at 0° and increases for larger angles. Above 600 MeV the PMT response becomes a maximum at 0°. The FWHM of the weighted average spectra are 5 to 15% larger than the 12° FWHM, except for 912 and 601 MeV where they are about 30% larger. For these proton beams the response FWHM are partly from the beam energy widths (see Table 2.3), so the 12° responses should still give a good first-order estimate of the HEPAD response to an omnidirectional proton flux.

The angular responses of the two HEPAD solid state detectors (refer to detector geometry in Fig. 2.2) are given in Table 3.2, where the responses are normalized to the TOF good proton counts.

Table 3.1

Summary of Data for HEPAD Angular Response for Protons

Angle and Characteristic	Response normalized to 12° peak for protons of energy						
	Rel. peak	912 MeV	601 MeV	561 MeV	474 MeV	412 MeV	368 MeV
0° - Peak/FWHM	1.20/0.24	1.17/0.23	1.03/0.29	0.84/0.32	0.82/0.35	0.86/0.49	0.85/0.81
- Avg/2.36 σ	1.23/0.31	1.18/0.33	1.04/0.30				
12° - (Peak)/FWHM	1.0/0.23	1.0/0.33	1.0/0.25	1.0/0.28	1.0/0.40	1.0/0.54	1.0/0.87
- Avg/2.36 σ	1.05/0.32	1.02/0.34	1.01/0.29				
24° - Peak/FWHM	0.97/0.23	0.82/0.21	0.79/0.21	0.90/0.31	1.01/0.34	1.16/0.42	1.25/0.81
Avg/2.36 σ	1.00/0.39	0.84/0.29	0.79/0.31				
Wtd Avg-Peak/FWHM	0.99/0.25	0.91/0.41	0.97/0.33	0.95/0.32	1.01/0.43	1.06/0.59	1.10/0.92
-Avg/2.36 σ	1.05/0.35	0.97/0.40	0.94/0.38				

Note 1: Data for Rel. peak, 912 MeV and 601 MeV are for HEPAD SN6 at HV42, taken at the BNL AGS in March, 1985. FWHM are also normalized to the 12° peak.

Note 2: Data for 561, 474, 412, and 368 MeV are from Ref. 2. The 24° listed results are averages of the 21° and 27° data.

The front detector (S1 counts) has the expected cos θ response to within 4%, while the rear detector (S2 counts) has a response that is 10% low at 12°, and 24% low at 24° and 36°. The front detector is shielded by 2.37 g/cm^2 of Al and 5.36 g/cm^2 of W at 0°. The proton range-energy tables of Ref. 5 include calculations of the probability of inelastic nuclear interactions. The calculations can be converted into a probability for inelastic nuclear interaction per g/cm^2 of material, and for 900 MeV protons this is 0.0090 for Al and 0.0054 for W. For the front detector at 0° this gives an interaction probability of 0.054 at 0°, but at other angles a part of the rear detector is shielded by the brass and ceramic mount of the front detector. At larger angles the rear detector is shielded by long particle pathlengths through the cylindrical Al and W side shields. An approximate calculation gives an inelastic interaction probability of about 0.14 at 30°, but shielding geometry is complicated and this is only an approximation. Since the inelastic interaction probability per g/cm^2 is probably also uncertain by a factor of 2, especially at 900 MeV, the rear detector angular response decrease at 12° to 36° is reasonably well explained by the increase in inelastic proton interactions in the detector shielding. The 0° response ratios correspond to a detector area of 2.98 cm^2 (S1/Good protons) and 3.00 cm^2 (S2/Good protons) if the TOF rear scintillator is taken as 2 inches in diameter. This is in excellent agreement with the nominal solid state detector areas of 3 cm^2.

The coincidence count response of the HEPAD is given in Table 3.3. S5 is the solid state detector coincidence pulse while the sum of all proton counts is the P1 + P2 + P3 + P4 count sum from the HEPAD. The external S5 counts were nearly identical to the internal (HEPAD) S5 counts, as expected (minor differences are due to slight threshold differences and statistical effects from pulses near the threshold level). The theoretical response of the solid state detector coincidence mode is

$$A(\theta) = 2r^2 \cos\theta \left(\cos^{-1} x - x\,(1-x^2)^{1/2}\right) \qquad (3.1)$$

where

$$x = D \tan\theta/(2r) \qquad (3.2)$$

This expression is for two detectors of equal radius r (= 0.977 cm for 3 cm^2 sensitive area), separated by a distance D (= 2.92 cm, for the HEPAD).

The angular response data for S5 are in reasonable agreement with the theoretical A (θ). The 23% increase at 24° is only 6% of the A (0) value, and is comparable to the uncertainties in the detector areas and separation. Part of the 24° response may be background from inelastically scattered protons, as shown by the non-zero response at 36°. The S5 response at 0° gives an experimental area of 2.62 cm^2, which is 88% of the S1 and S2 areas.

The HEPAD proton count response is given in the second part of Table 3.3. The sum of all proton counts relative to the good proton gates from the TOF system measures the effective HEPAD response, which is set by the fast triple coincidence (2 SSDs +

Table 3.2

Angular Responses of HEPAD Solid State Detectors

HEPAD SN6 at HV 42

A) Front Detector Response - S1 counts

Angle θ(deg)	S1/(Good protons) for protons of Rel. Peak	912 MeV	601 MeV	Average S1 Response	Normalized S1 Response/cosθ
0	0.151	0.145	0.146	0.147	≡1.00
12	0.149	0.144	0.143	0.145	1.01
24	0.138	0.133	0.136	0.136	1.01
36	0.125	0.123	0.124	0.124	1.04

B) Rear Detector Response - S2 counts

Angle θ(deg)	S2/(Good protons) for protons of Rel. Peak	912 MeV	601 MeV	Average S2 Response	Normalized S2 Response/cosθ
0	0.156	0.147	0.141	0.148	≡1.00
12	0.142	0.131	0.118	0.130	0.90
24	0.103	0.105	0.102	0.103	0.76
36	0.101	0.084	0.089	0.091	0.76

Table 3.3

Angular Response of HEPAD Coincidence Counts

HEPAD SN6 at HV42

A) Solid State Detector Coincidences - S5 counts

Angle θ(deg)	S5/(Good protons) for protons of Rel. Peak	912 MeV	601 MeV	Average S5 Response	Theory A (θ)(cm^2)	Normalized S5 Response/A(θ)
0	0.131	0.128	0.129	0.129	3.000	≡1.00
12	0.0884	0.0841	0.0765	0.0830	1.767	1.09
24	0.0355	0.0303	0.0299	0.0319	0.604	1.23
36	0.0075	0.0032	0.0040	0.0049	-	-

B) HEPAD Proton Counts - Sum of all proton counts (P1 + P2 + P3 + P4)

Angle θ(deg)	(Sum P)/(Good protons) for protons of Rel. Peak	912 MeV	601 MeV	Average P response	Normalized P response/A(θ)
0	0.1174	0.1182	0.1192	0.1183	≡1.00
12	0.0771	0.776	0.0689	0.0745	1.07
24	0.0280	0.0263	0.0257	0.0267	1.12
36	0.0023	0.0009	0.0007	0.0013	-

PMT) in the HEPAD. The shape of the angular response is in good agreement with the theoretical response, while the average 0° response corresponds to 2.40 cm^2 relative to a two inch diameter TOF rear scintillator. This response is 80% of the S1-S2 response.

The HEPAD total geometric factor is given by

$$G = -\frac{\pi^2}{2}- (2r^2 + D^2 - D(4r^2 + D^2)^{1/2}) \qquad (3.3)$$

$$= 0.869 \ cm^2 - sr$$

for r = 0.977 cm and D = 2.92 cm. With the triple coincidence giving an 80% response relative to the S1-S2 0° area of about 3 cm^2, the effective geometric factor of the HEPAD is

$$G_{eff} \simeq 0.80 \ G$$

$$= 0.695 \ cm^2-sr \qquad (3.4)$$

The value of G_{eff} allows for the particle losses associated with the fast triple coincidence circuitry.

The angular distribution data show that the 12° HEPAD response can be used to obtain a calibration curve which should be accurate to 5% in the PMT pulse height. Because of the non-linear output of Cerenkov light vs. proton energy and the 25 to 30% FWHM of the PMT response, the 5% calibration curve accuracy should not have a significant effect on proton spectra calculation from the HEPAD data. Using the 12° HEPAD response for calibration significantly reduces the amount of data and the analysis effort required to obtain the experimental HEPAD calibration.

3.2 HEPAD Response to Atmospheric Muons

Atmospheric muon data were obtained with HEPAD SN6 at HV42 in July 1984 and March 1985 as listed in Table 2.4. The results, all normalized to the atmospheric muon peak, are listed in Table 3.4. The alpha lamp peak is 0.261 of the muon peak, with an accuracy of ±3%. The alpha lamp has a FWHM of about 50% with the average pulse height about 1.061 times the peak, so the spectral shape is slightly asymmetric. The measured atmospheric muon spectrum is plotted in Fig. 3.1, along with the BNL AGS relativistic peak spectra for 12° and for the Wtd Avg, calculated as described in Section 3.1. The spectral shapes are similar, although the atmospheric muon spectrum peak is about 6% lower than the 12° relativistic peak. This normalization difference is discussed in more detail in Section 3.3.

The total atmospheric muon count rate, measured as the summed proton channel counts (P1 + P2 + P3 + P4), was quite constant, being 0.617 ± 0.011, 0.617 ± 0.013, and 0.616 ± 0.026 counts/minute for 7/84, 3/11-14/85, and 3/25-26/85. The atmospheric muon count rate varies with geomagnetic location, and can be affected by strong solar activity. Measurements at PI in

Table 3.4

Atmospheric Muon Data Results from HEPAD SN6 at HV 42

All results are normalized to the peak of the atmospheric muon spectrum.

Item measured	Values normalized to muon peak for 7/16-20/84	3/11-14/85	3/25-26/85	Average value
α pk/FWHM	0.270/0.136	0.262/0.132	0.252/0.124	0.261/0.131
α avg/2.36 σ	0.285/0.152	0.279/0.150	0.268/0.145	0.227/0.149
mu pk/FWHM	1.000/0.319	1.000/0.266	1.000/0.293	1.000/0.293
mu avg/2.36 σ	1.051/0.376	1.024/0.286	1.040/0.341	1.038/0.334
LS1 (S3, P1)	0.085	0.071	0.080	0.079
LS2 (S4,P1,P2)	0.366	0.375	0.367	0.369
LS3 (P2, P3)	0.603	0.630	---	0.617
LS4 (P3, P4)	0.823	0.807	---	0.815

Note: for Average Values: FWHM/α peak = 0.502

2.36 σ/α avg = 0.538

α avg/α peak = 1.061

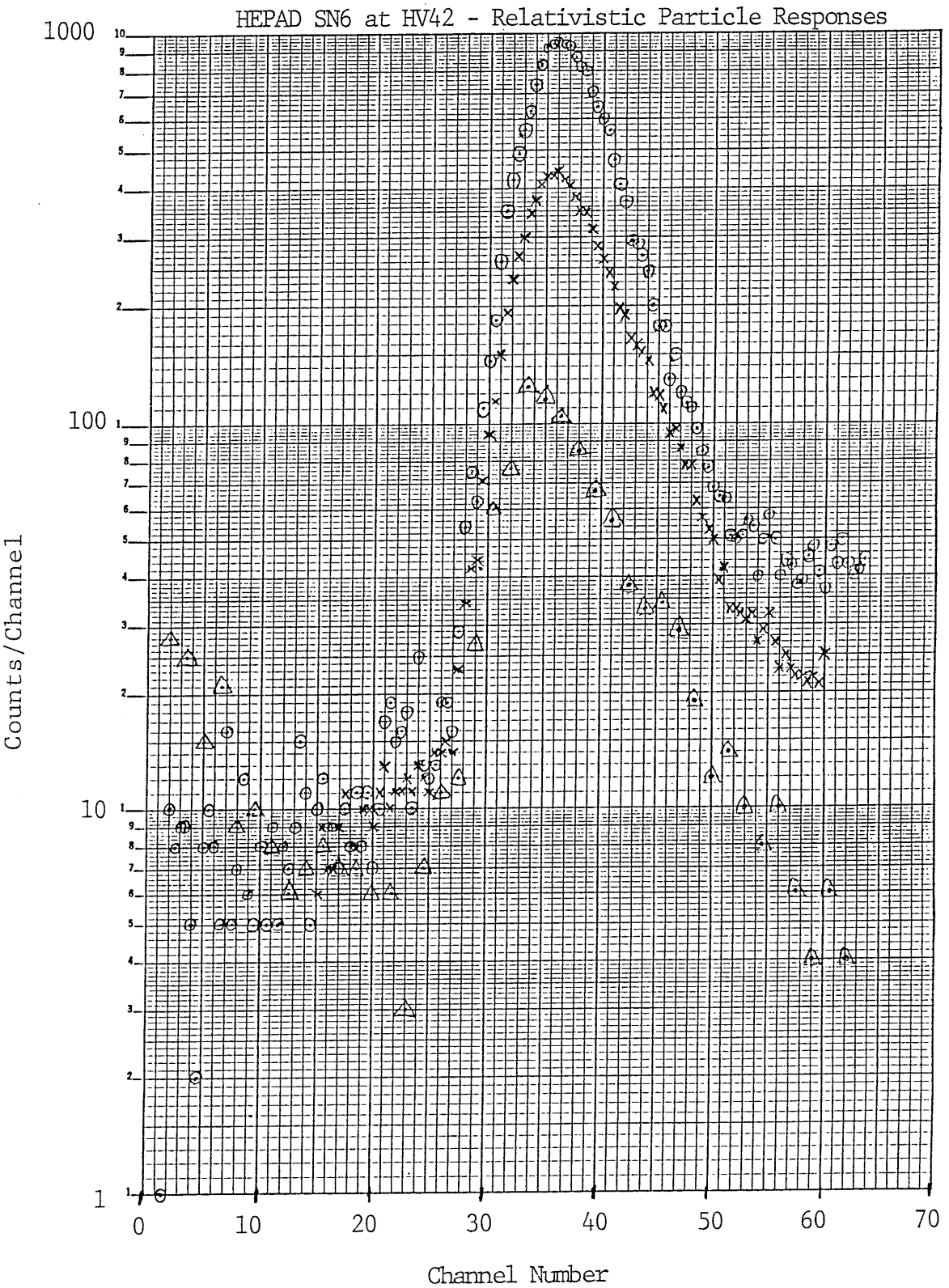

Figure 3.1. HEPAD SN6 at HV42, Atmospheric Muon Spectrum, and BNL AGS Relativistic Peak Spectra at 12° and Wtd. Avg.

Waltham, MA, can be compared for periods of comparable solar activity, i.e. no ground-level-events (GLEs) from high energy solar proton emission. The SN6 atmospheric muon run proton count data show stable operation from 7/84 to 3/85.

The measured values for the four proton thresholds on the PMT, LS1-LS4, are also listed in Table 3.4. These are obtained from muon run spectra taken in coincidence with P1-P4, as shown for each level. The S3, S4 runs use the alpha lamp spectrum to obtain LS1 and LS2. For P1-P3 the zenith view muon runs require long times because only the weak, low pulse height tail is being used. Nadir view muon runs provide good threshold data for P1-P3 in a shorter time period.

Atmospheric muon run data for HEPAD SN9 are shown in Table 3.5, for the time periods listed in Table 2.5. SN9 was received from NOAA in December 1984, and for the initial muon run testing the normal buffer amplifier for the PMT DY10 pulse was not available (it was being used with SN6 in the EPS SN4 Acceptance Testing). For the 12/17-27/84 period an oscilloscope preamplifier was used, the HEPAD DY10 cable being longer than normal. On 12/17/84 a different DY10 buffer amplifier and shorter cable were used, and this changed the data, as can be seen by the abrupt change in α/muon peak ratio. Later checks proved unable to reproduce the 12/17-27/84 data, even with the oscilloscope amplifier. The final conclusion is that there was some malfunction in the oscilloscope amplifier, possibly associated with the scope triggering and/or with a poor electrical contact on the rotary gain switch. Thus, the data for 12/17-27/84 have not been used to derive the average values for the several parameters listed in Table 3.5.

Intitial SN9 data were taken at HV36, while the BNL data indicated that HV34 is better. The drop of 2 HV steps corresponds to a decrease of 9% in the DY10 signal amplitude (measured), which corresponds to about a 10% increase in all LS level values relative to the muon peak. Note that LS1 comes form the anode (A) signal, LS2-LS4 from DY12, and LS5-LS6 from DY11. An analysis of signal gains from the added dynode amplification gives the 10% change for all levels (A, DY12, DY11) within a fraction of 1%. It should be noted that variations of the PMT gain and of the threshold firing levels are generally a few % for normal room temperature variations, HEPAD warm-up, and humidity variations, so the LS level accuracies are in the range of $\pm$ a few %.

The initial alpha lamp setting was well above LS2 (S4), so the S4/S3 ratio was a poor monitor of the PMT gain at the desired level of HV34. The alpha lamp was adjusted on 7/17/85, the final α/muon ratio being given in the 7/17-23/85 data in Table 3.5. This adjustment does not affect the LS level ratios to the atmospheric muon peak. Characteristics of the alpha lamp data are summarized in Table 3.6. Note that the SN9 alpha lamp spectrum is less asymmetric than the SN6 alpha lamp, and is about 20% narrower in FWHM.

An S5 coincidence atmospheric muon spectrum for HEPAD SN9 is shown in Fig. 3.2. This shows the high pulse height tail, the

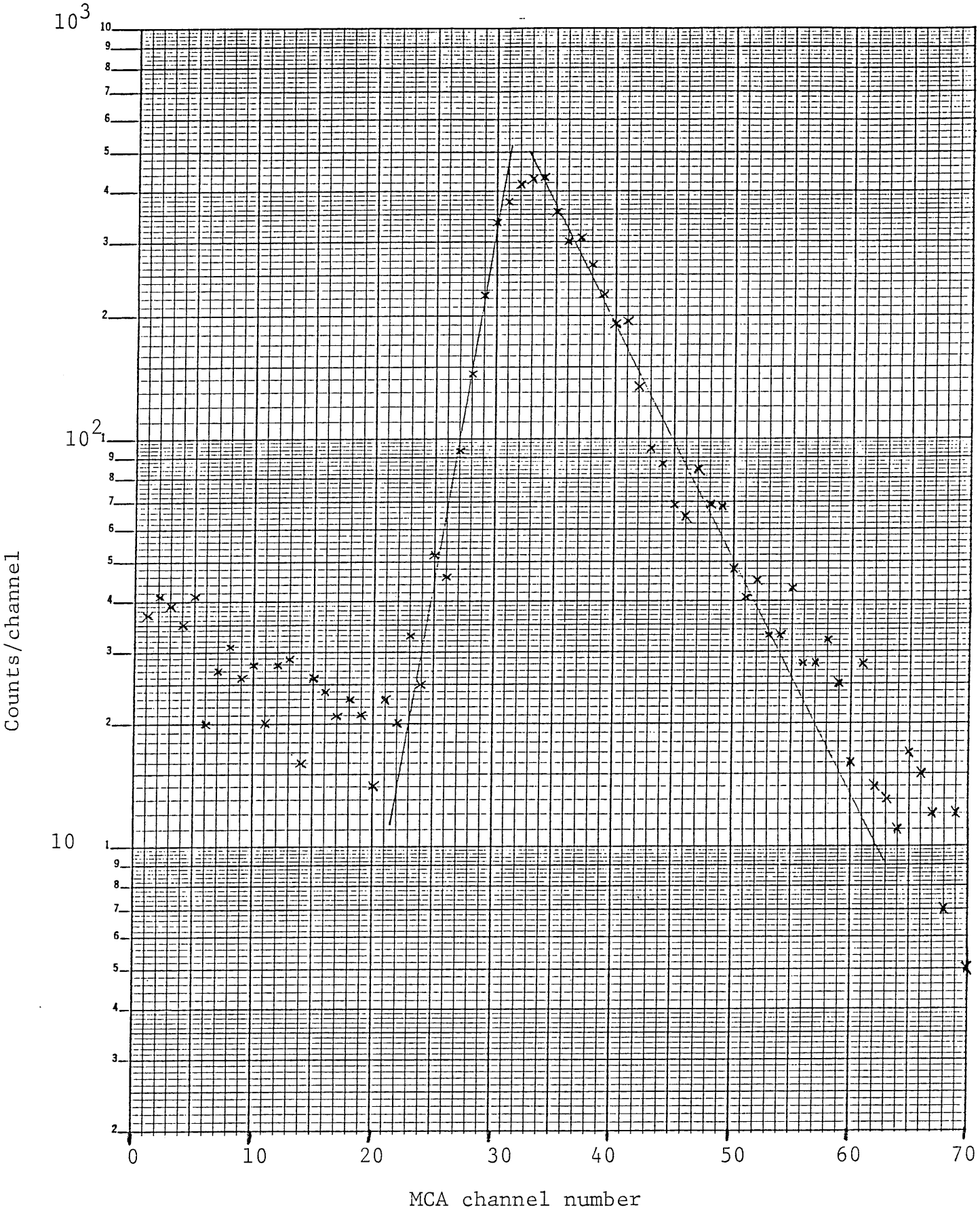

Figure 3.2. Atmospheric Muon Spectrum from HEPAD SN9-S 5 Coincidence

Table 3.5

Atmospheric Muon Data Results from HEPAD SN9 Normalized to HV34

All results are normalized to the peak of the atmospheric muon spectrum.

Item Measured	Values normalized to muon peak for								
	12/17-27/84*	12/28-1/17/85	3/26-4/1/85	5/1-6/85	5/17-20/85	6/3-5/85	7/2-17/85	7/17-23/85+	Average
pk/FWHM	0.490/0.168	0.407/0.151	0.367/0.131	0.382/0.132	0.369/0.132	0.399/0.145	0.390/0.144	0.324/0.136	0.386/0.139
avg/2.36	0.495/0.172	0.409/0.147	0.374/0.132	0.389/0.138	0.374/0.136	0.405/0.153	0.398/0.151	0.333/0.140	0.392/0.143
mu pk/FWHM	1.000/0.154	1.000/0.307	1.000/0.342	1.000/0.295	1.000/0.292	1.000/0.309	1.000/0.293	1.000/0.271	1.000/0.303
mu avg/2.36	1.031/0.264	1.079/0.407	1.037/0.342	1.056/0.336	1.048/0.334	1.059/0.360	1.053/0.354	1.051/0.356	1.055/0.356
LS1 (S3,P1)	0.063	-	-	0.052	0.049	0.065	0.064	0.057	0.057
LS2 (S4,P1,P2)	0.384	-	0.301	0.318	0.306	0.317	0.317	0.323	0.314
LS3 (P2,P3)	0.692	-	0.518	0.525	-	-	0.543	0.514	0.525
LS4 (P3,P4)	0.856	0.739	0.695	0.722	0.729	0.705	0.743	0.736	0.724
LS5 (P4,A1)	1.98	2.63	-	-	-	-	-	-	2.63(=4x0.658)
LS6 (A1,A2)	-	3.09	-	-	-	-	-	-	3.09(=4x0.773)

*12/17-27/84 data not included in average - see text.

+7/17-23/85 data are after the final alpha lamp adjustment.
The alpha lamp part of the data are not used in the average.

Table 3.6

HEPAD SN9 Alpha Lamp Data

Characteristics at initial setting:

Ratios to atmospheric muon peak

α pk/FWHM	0.386/0.139
α avg/2.36 σ	0.392/0.143

FWHM/α pk = 0.360
2.36 σ/α avg = 0.365

α avg/α pk = 1.016

Characteristics at final setting:

Ratios to atmospheric muon peak

α pk/FWHM	0.324/0.136
α avg/2.36 σ	0.333/0.140

FWHM/α pk = 0.420
2.36 σ/α avg = 0.420

α avg/α pk = 1.028

sharp edge on the low pulse height side of the peak, and the low pulse height background. The atmospheric muon peak for SN9 is about 8% higher than the 12° relativistic peak measured at BNL, using the alpha lamp for normalization. This is opposite to the shift measured in SN6.

The data in Table 3.5 show a variation in α pk/mu pk of ±5%, which is partly from uncertainty in selecting the peak of the muon spectrum.

The atmospheric muon count rates for HEPAD SN9 for several periods are listed in Table 3.7. Zenith and Nadir count rates are expected to be different. The variations in Zenith count rate comes from capacitor and ±6V supply problems discussed in Section 2.2. The final count rate for SN9 in 7/85 was 0.624 ± 0.008, in excellent agreement with the SN6 data. Thus, both HEPADs show the same detection efficiency for atmospheric muons, when all circuitry and power supply voltages are properly adjusted.

The ratio of the atmospheric muon peak to the BNL relativistic muon peak at 12° averages to 1.00 with an uncertainty of about ±5%. For the analysis of the 12° proton data from BNL, the 12° relativistic peak will be taken as equal to the atmospheric muon peak. This is consistent with the angular distribution results discussed in Section 3.1. The HEPAD PMT gain variation with environmental conditions makes it difficult to obtain measurements

TABLE 3.7

Atmospheric Muon Run Count Rates for Proton Channel Sum - HEPAD SN9

Date Range	Zenith or Nadir	Proton Sum Count Rate (cuts/min)
12/17-20/84	Zenith	0.645 ± 0.013
12/20-26/84	Nadir	[0.460 ± 0.007]
12/28/84-1/2/85	Zenith	0.584 ± 0.009
1/2-17/85	Zenith	0.633 ± 0.005
3/26-29/85	Zenith	0.572 ± 0.012
5/2-6/85	Zenith	0.582 ± 0.011
5/17-24/85	Zenith	0.620 ± 0.011
6/3-5/85	Zenith	0.573 ± 0.015
7/12-22/85	Zenith	0.624 ± 0.008
7/23/85	Nadir	[0.459 ± 0.020]

more accurate than ± 3%. The atmospheric muon calibration and the BNL 12° relativistic beam calibration are equal to within ±5%, and this is about the best accuracy that can be readily achieved for an absolute HEPAD calibration.

3.3 HEPAD Calibration with Protons at 12°

HEPADs SN6 and SN9 were calibrated with protons at 12°, with data obtained for the energies listed in Tables 2.1 and 2.2. HEPAD particle counts were obtained for all energies, and DY10 spectra for most energies. The geometric factors for the four proton channels were calculated from

$$A\ (Pi,\ 12^{o}) = A\ (S1,\ 12^{o}) \times Cnt\ (Pi)/Cnt\ (S1) \qquad (3.5)$$

where

$$A\ (S1,\ 12^{o}) = 3.00 \cos 12^{o}$$

$$= 2.93\ cm^2$$

From eq. (3.1) and Table 3.3 the theoretical value for A (Pi, 12°) = 1.767 cm^2, maximum, with this value actually applying to the sum of the four proton channel areas.

The measured proton channel areas at 12° for HEPAD SN6 at HV42 are listed in Table 3.8 and plotted in Fig. 3.3. The statistical errors for some of the measurements are also shown in Fig. 3.3. The measured value for the P Sum area above about 450 MeV is 1.504 cm^2, which is 85% of the theoretical value, and is thus the efficiency of the fast triple coincidence in the HEPAD. The effective geometric factor of HEPAD SN6 for high energy protons is, therefore, 0.740 cm^2-sr, using eqs. (3.3) and (3.4) with a 0.851 efficiency.

The measured areas for HEPAD SN9 at HV34 are given in Table 3.9 and Fig. 3.4. The measured P Sum area for 400 - 700 MeV protons is 1.23 cm^2 (70% efficiency), while for energies above 800 MeV it is 1.00 cm^2 (57% efficiency). This decreased efficiency is the result of DC offsets in the solid state detector signals to the fast coincidence circuitry, which was caused by the leaking capacitor and different ±6V supply voltages. The lower efficiency at high proton energies is consistent with the lower energy loss of these protons, causing problems with the solid state detector pulses. The data from HEPAD SN9 are valid for obtaining the relative channel reponses and the PMT response, but the absolute efficiency is too low. The repaired HEPAD should have the same efficiency as SN6, since the atmospheric muon count rates at PI were measured to be the same (see end of Section 3.2).

Table 3.8

Measured Proton Channel Areas at 12° for HEPAD SN6 at HV42

Proton Energy (MeV)	Measured areas at 12°, in cm^2, for Channel P1	Channel P2	Channel P3	Channel P4	Summed P Channels
Rel. Peak	0.004	0.006	0.017	1.456	1.483
1160	0.004	0.011	0.229	1.259	1.503
1024	0.006	0.026	0.332	1.151	1.515
883	0.004	0.027	0.461	1.093	1.585
760	0.006	0.034	0.749	0.749	1.538
695	0.027	0.087	0.926	0.363	1.403
626	0.015	0.182	1.123	0.167	1.487
560	0.000	0.740	0.856	0.029	1.625
540	0.034	1.042	0.492	0.057	1.625
495	0.047	1.235	0.111	0.024	1.417
460	0.169	1.208	0.042	0.036	1.455
438	0.474	0.869	0.000	0.016	1.359
407	1.122	0.200	0.000	0.047	1.369
397	1.135	0.179	0.000	0.047	1.361
362	1.044	0.000	0.005	0.034	1.083
336	0.377	0.003	0.000	0.067	0.447
307	0.045	0.000	0.005	0.083	0.133

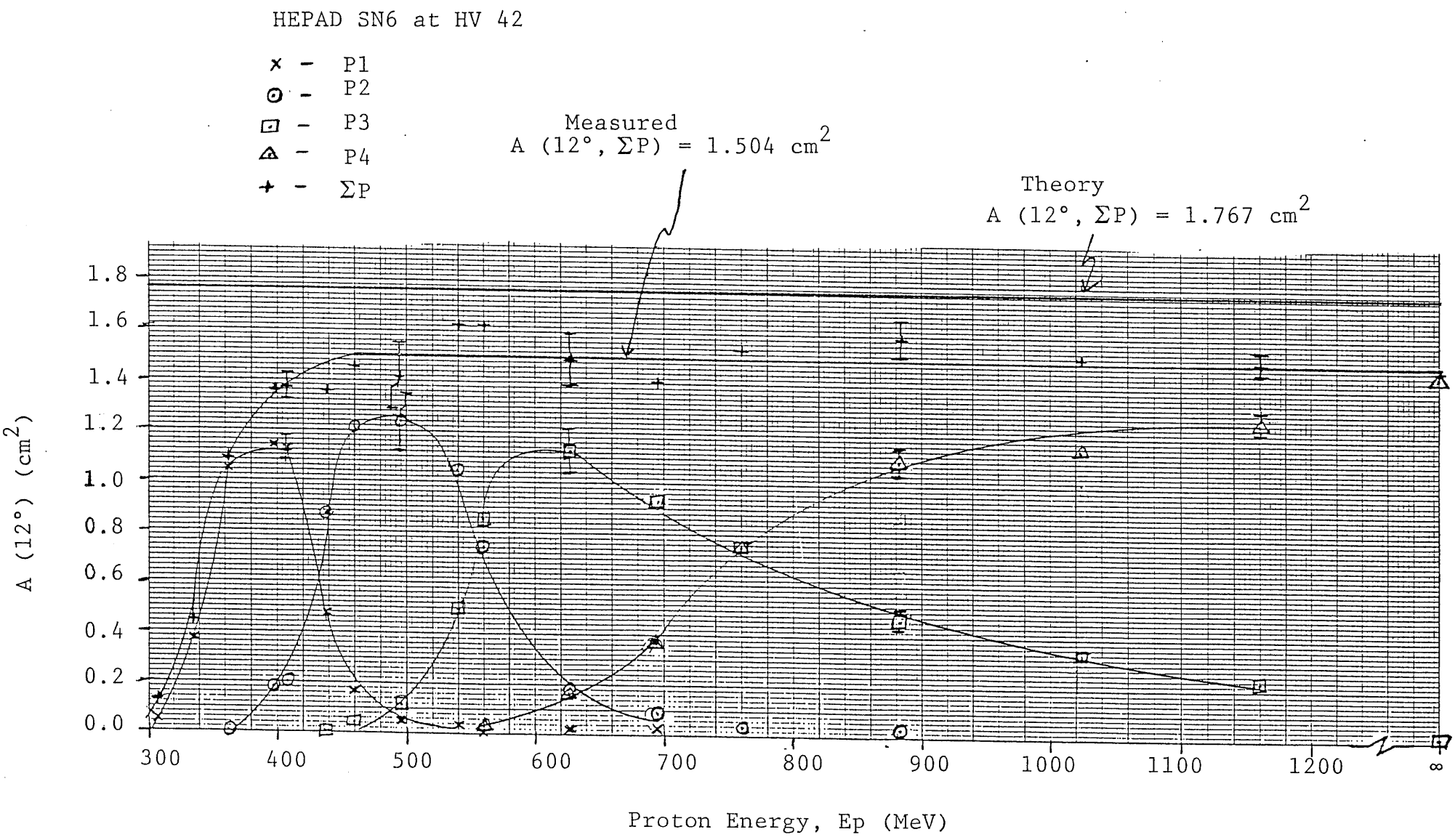

Figure 3.3. Plot of Measured Proton Channel Area at 12° for HEPAD SN6 at HV42

Table 3.9

Measured Proton Channel Areas at 12° for HEPAD SN9 at HV34

Proton Energy (MeV)	Measured areas at 12°, in cm^2, for Channel P1	Channel P2	Channel P3	Channel P4	Summed P Channels
Rel.Pk.(HV36!)	0.005	0.003	0.004	1.011	1.023
932	0.007	0.013	0.284	0.658	0.962
807	0.008	0.011	0.423	0.575	1.017
764	0.013	0.017	0.556	0.543	1.129
693	0.008	0.039	0.800	0.381	1.228
629	0.014	0.093	0.987	0.180	1.274
582	0.018	0.281	0.940	0.032	1.271
542	0.012	0.501	0.655	0.012	1.180
494	0.021	0.986	0.182	0.021	1.210
442	0.374	0.860	0.000	0.028	1.262
400	1.159	0.076	0.003	0.015	1.253
370	1.148	0.004	0.000	0.023	1.175
343	0.714	0.000	0.000	0.022	0.736
315	0.152	0.000	0.000	0.013	0.165

The proton channel response curves for SN6 and SN9 are in reasonable agreement. Note the wide energy range of the P3-P4 transition at 700-800 MeV. At lower energies the transitions are sharper. The transition energies and level values corrected to the 12° relativistic peak (x 1.065 for HEPAD SN6, x 0.928 for HEPAD SN9) are listed in Table 3.10.

The level setting for 50% detection of a given proton energy can also be obtained from the PMT DY10 spectra. By using the SN6 and SN9 MCA spectra listed in Tables 2.1 and 2.2, a more extensive set of calibration points can be obtained. Tables 3.11 and 3.12 list the resulting data, along with information on the FWHM, 2.36σ (calculated FWHM), and the difference between the average and the peak. The (1/2 count P.H.)/(Rel. Peak) gives the effective threshold value for the listed proton energy, normalized to the 12° relativistic peak.

The proton energy vs. threshold data are plotted in Fig. 3.5, along with the 12° measurements of Ref. 2. The Ref. 2 data have been normalized to the atmospheric muon peak, which they found to be 16% lower than expected based on the proton data. The extra curves in Fig. 3.5 show the $\pm$ 1σ spread from the PMT response, obtained from the data in Tables 3.11 and 3.12 corrected for the beam energy width. The data all show good agreement, and the center curve can be used as the HEPAD calibration curve for an omnidirectional beam, accurate to at least $\pm$ 5%. The $\pm$ 1σ curves can be used to estimate the energy spread for a given threshold, although it should be noted that high energy protons have a long tail on the high energy side of the threshold (see relativistic particle spectra in Figs. 3.1 and 3.2).

The HEPAD calibration curve in Fig. 3.5 differs somewhat from the earlier calibration curve in Refs. 3 and 4. This is most likely the result of higher energy proton contamination of the TOF beam in the March 1980 HEPAD data, as discussed in Section 3.1. The HEPAD calibration curve in Fig. 3.5 should be quite accurate since all spurious peaks in the TOF system were eliminated, and there is good agreement between the BNL AGS data and the data of Ref. 2. The curves in Fig. 3.5 should also apply to calibration relative to the atmospheric muon peak, to within $\pm$ 5%.

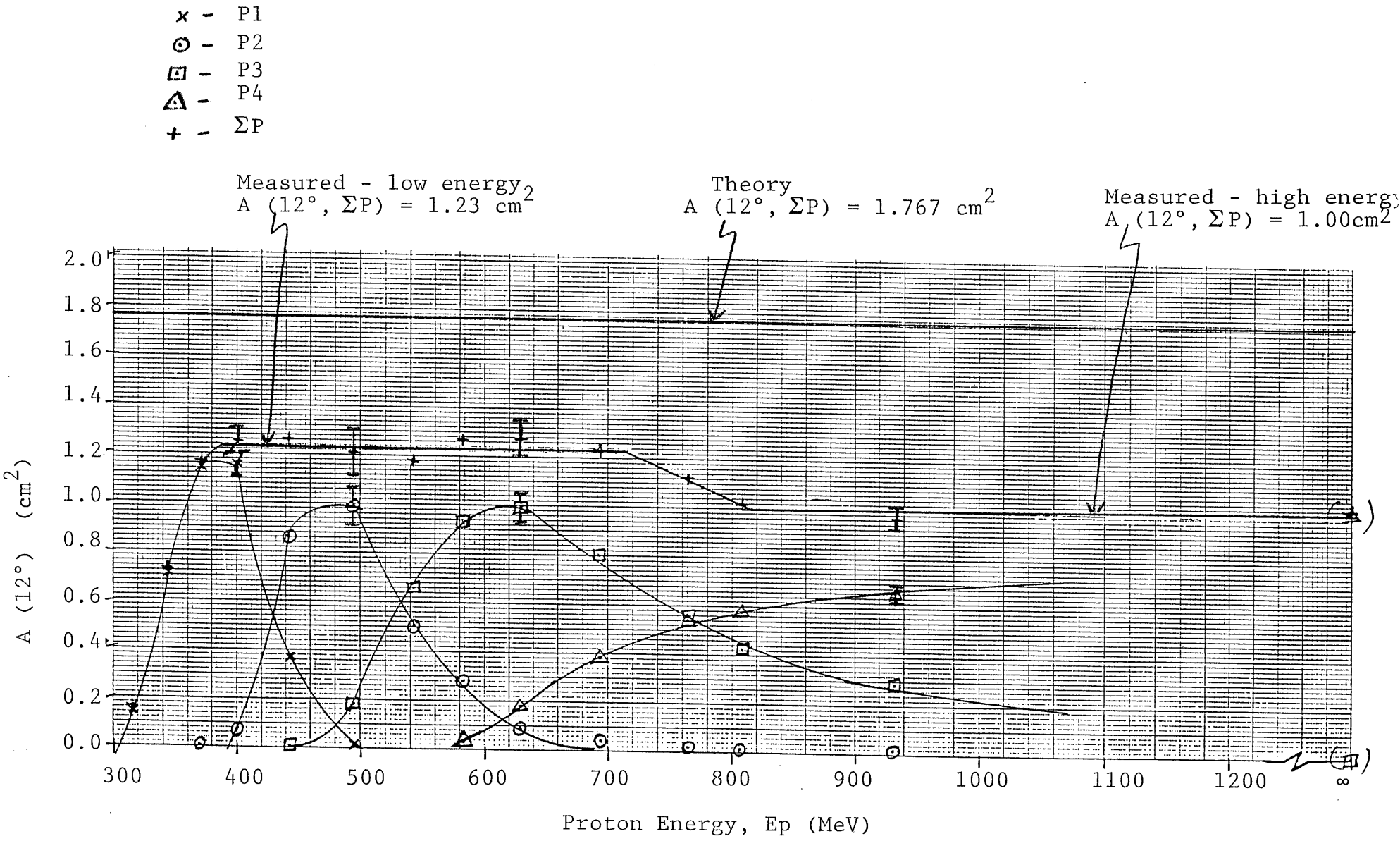

Figure 3.4. Plot of Measured Proton Channel Areas at 12° for HEPAD SN9 at HV 34

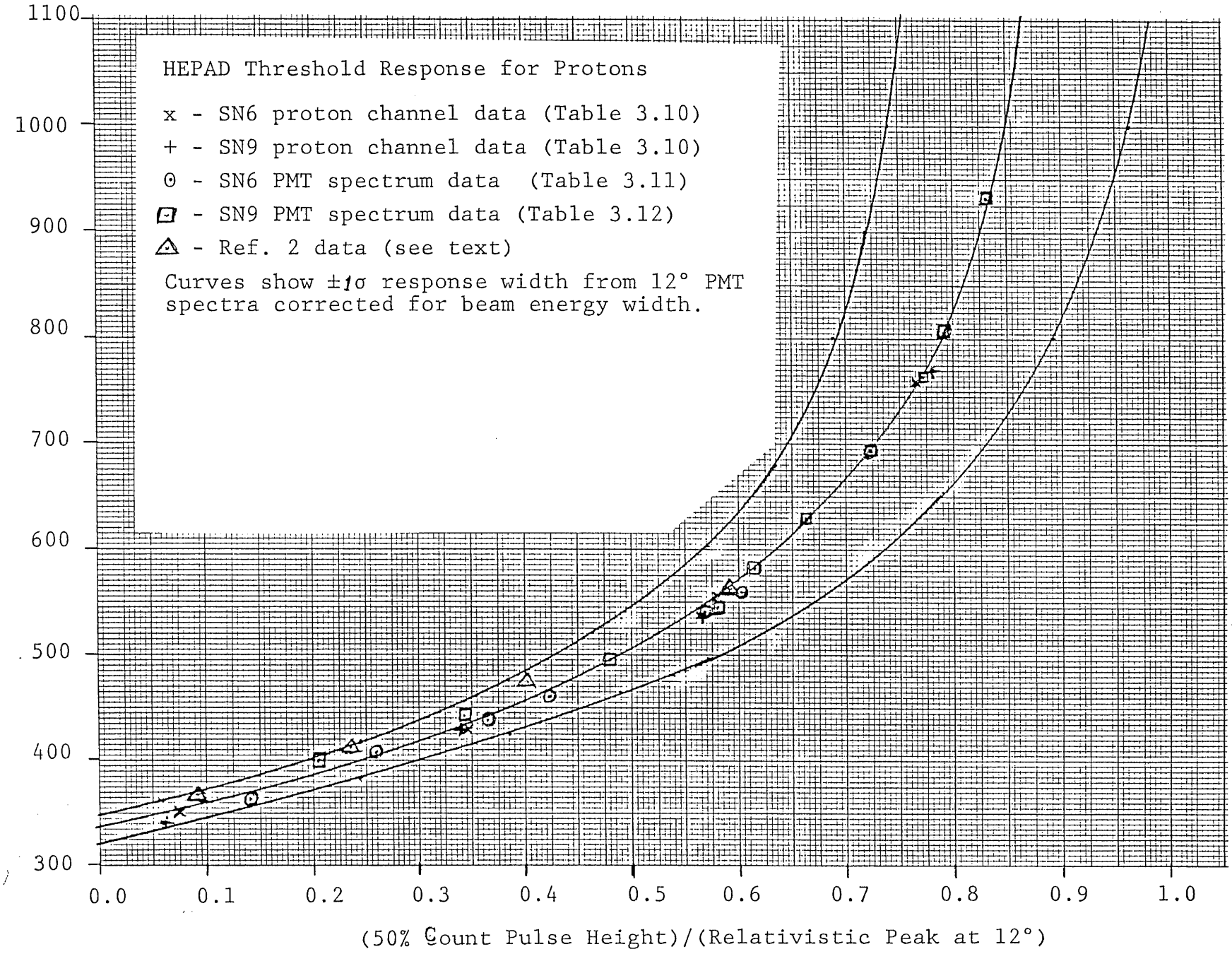

Figure 3.5. Proton Energy vs. Threshold for the HEPAD at 12°

Table 3.10

Proton Channel Transition Energies and Level Values

Normalized to the 12° Relativistic Peak

	SN6 Data		SN9 Data	
Level Designation	Level Value[1]	Transition Energy (MeV)	Level Value[2]	Transition Energy
LS1	0.074	350	0.061	340
LS2	0.346	430	0.338	430
LS3	0.579	555	0.566	535
LS4	0.765	760	0.780	770

1) Average level values from Table 3.4 divided by 1.065, the measured ratio of the 12° relativistic peak and the atmospheric muon peak for SN6.

2) Average level values from Table 3.5 divided by 0.928, the measured ratio of the 12° relativistic peak and the atmospheric muon peak for SN9.

Transition energies taken from Figs. 3.3 and 3.4.

Table 3.11

PMT Spectrum Measurement Results for Protons at 12°, HEPAD SN6 at HV42

Proton Energy (MeV)	Relative Peak Pulse Height	$\left(\frac{\text{Peak}}{\text{Average}}\right)\left(\frac{2.36\sigma}{\text{Avg}}\right)$		$\left(\frac{\text{FWHM}}{2.36\sigma}\right)$	$\left(\frac{\text{1/2 Count P.H.}}{\text{Rel. Peak}}\right)$
Rel. Pk.	≡1.000	0.969	0.290	0.826	1.021
695	0.706	0.963	0.342	---	0.723
560	0.610	1.007	0.283	---	0.603
540	0.562	0.993	0.262	---	0.567
460	0.418	0.993	0.433	1.090	0.422
438	0.363	1.000	0.509	0.889	0.366
407	0.253	0.989	0.701	1.031	0.260
362	0.117	0.876	0.887	1.047	0.141

Table 3.12

PMT Spectrum Measurement Results for Protons at 12°, HEPAD SN9 at HV34

Proton Energy (MeV)	Relative Peak Pulse Height	$\left(\frac{\text{Peak}}{\text{Average}}\right)\left(\frac{2.36\sigma}{\text{Avg}}\right)$		$\left(\frac{\text{FWHM}}{2.36\sigma}\right)$	$\left(\frac{\text{1/2 Count P.H.}}{\text{Rel. Peak}}\right)$
Rel. Pk.	≡1.000	0.965	0.284	0.826	---
932	0.810	0.963	0.294	0.893	0.831
807	0.781	0.983	0.298	0.897	0.791
764	0.766	0.990	0.280	1.020	0.769
693	0.714	0.986	0.297	0.822	0.720
629	0.655	0.980	0.293	0.827	0.663
582	0.619	1.002	0.289	0.826	0.614
542	0.582	1.013	0.279	1.009	0.579
494	0.471	0.979	0.343	0.893	0.480
442	0.346	1.022	0.426	0.765	0.342
400	0.191	0.929	0.793	0.946	0.205

3.4 HEPAD Response to Rear Entry Particles

The HEPAD response to high energy, rear entry protons was measured with SN6 as listed in Table 2.3. The angular responses of the solid state detectors, including the S5 coincidence, are listed in Table 3.13. The S1 and S2 responses are slightly low, primarily because of scattering and inelastic interactions in the shielding from the PMT, electronics, and housing. The S5 response is low at 180°, but high at 156° and 144° because of scattering. The solid state detector responses are consistent with the front entry measurements, and are in rough agreement with the expected response when scattering and inelastic interactions are considered.

The HEPAD proton channel responses are listed in Table 3.14, where the total geometric factors for P1 and P2 are given. The P1 response to the relativistic peak is almost flat, while all the other responses peak near 156°. The P1 response falls off rapidly at 600 MeV, while the P2 response is already low at 900 MeV. The P3 and P4 channel responses are well below the P2 response and can be neglected. The PMT spectra show a similar response, the pulse height being a maximum near 156°. The weighted average PMT spectra are plotted in Fig. 3.6, and show the HEPAD response to an omnidirectional particle flux from the rear. The thresholds LS1-LS4, which determine P1-P4, are also shown in Fig. 3.6. The low values at high pulse heights have large statistical errors because of low counts. The high energy tails may be contaminated by response to scattered and interacting particles.

The HEPAD PMT nadir view response to atmospheric muons is shown in Fig. 3.7. The data were taken with HEPAD SN9 at HV 34, and the values of LS1-4 (P1-P4) for SN9 and SN6 (at HV 42) are also shown. The P1-P4 count results for the nadir view muon run are given in Table 3.15, where the counts rates are converted to G_{nadir} (cm^2-sr) for each channel, normalizing to 0.624 cpm for the zenith view atmospheric muon runs, and using 0.740 cm^2-sr as the effective total geometric factor for zenith view atmospheric muons. The 0.740 cm^2 is based on a triple coincidence efficiency of 0.851, as measured for HEPAD SN6 at HV 34 for protons above 450 MeV at 12° (see Section 3.3). The count ratios P1-P4 for SN9 and SN6, calculated from the PMT spectrum in Fig. 3.7, were then used to convert the SN9 data to equivalent G_{nadir} values for SN6 (with slightly different LS1-4 values). The resulting ratios of G (Rel.Pk)/G_{nadir} for SN6, using the Rel.Peak geometric factors measured for SN6 at BNL, are listed in the final column of Table 3.15. The agreement of P1 and P2 is excellent, and shows that rear entry particle response can be readily measured with nadir view atmospheric muon runs. The P3 and P4 results are different by about a factor of 2, but this comes from the large fractional errors of small counts and from possible background contamination of the small geometric factors.

Table 3.13

Rear Entry Particle Angular Responses of HEPAD Solid State Detectors

HEPAD SN6 at HV 42

A) S1 counts - Front Detector (for normal particle entry)

Angle θ(deg)	S1 area using 20.3cm^2 for (Good protons) Rel. Peak	900 MeV	600 MeV	269 MeV	Theory ($-3\cos\theta$)
180	2.78	2.54	2.50	2.38	3.000
168	2.72	2.46	2.42	---	2.934
156	2.74	2.50	2.50	---	2.741
144	2.50	2.29	---	---	2.427

B) S2 counts - Rear Detector (for normal particle entry)

Angle θ(deg)	S2 area using 20.3cm^2 for (Good protons) Rel. Peak	900 MeV	600 MeV	269 MeV
180	2.64	2.56	2.56	2.40
168	2.40	2.19	2.21	---
156	2.23	2.03	1.95	---
144	1.97	1.72	---	---

C) S5 counts - Coincidence Response

Angle θ(deg)	S5 area using 20.3cm^2 for (Good protons) Rel. Peak	900 MeV	600 MeV	269 MeV	A (θ) Eq. (3.1)
180	1.88	2.13	2.21	2.07	3.000
168	1.28	1.29	1.35	---	1.767
156	0.670	0.574	0.540	---	0.604
144	0.185	0.077	---	---	---

Table 3.14

Rear Entry Particle Responses of HEPAD
P1 and P2 Channels

HEPAD SN6 at HV 42

A) P1 Channel Response

Angle θ(deg)	P1 channel area (cm^2) from (Good protons) Rel. Peak	900 MeV	600 MeV	269 MeV
180	0.316	0.098	0.046	0.014
168	0.393	0.195	0.047	---
156	0.350	0.445	0.157	---
144	(0.042)	(0.027)	---	---
G(cm^2-sr)	0.305	0.294	0.098	---

B) P2 Channel Response

Angle θ(deg)	P2 channel area (cm^2) from (Good protons) Rel. Peak	900 MeV	600 MeV	269 MeV
180	0.029	0.0014	<0.001	<0.001
168	0.037	0.0015	<0.001	---
156	0.131	0.0027	<0.001	---
144	(0.015)	(0.0023)	---	---
G(cm^2-sr)	0.081	0.0019	<0.0009	---

Note: G (cm^2-sr) is calculated only from the 180°, 168°, and 156° data.

Table 3.15

Nadir View Atmospheric Muon Responses of HEPAD

Data from HEPAD SN9 at HV34, 7/22-23/85

Proton Channel	SN9 at HV34 Measured Response (cpm)	SN9 at HV34 G_{nadir} (cm^2-sr) a)	SN6 at HV42 Corrected (cm^2-sr) b)	SN6 at HV42 G (Rel Pk) c) / G_{nadir}
P1	0.315 ± 0.016	0.374	0.316	0.97
P2	0.095 ± 0.009	0.112	0.091	0.89
P3	0.022 ± 0.004	0.026	0.026	0.50
P4	0.027 ± 0.005	0.032	0.024	0.58

a) Calculated from a zenith view atmospheric muon total count rate of 0.624 ± 0.008 cpm, and a total geometric factor of 0.740 cm^2-sr (Section 3.3, SN6 results).

b) Calculated from the SN9 PMT spectrum and the LS1-4 values for SN9 and SN6. Count ratios were used to correct G_{nadir} of SN9.

c) G (Rel. Pk.) for SN6 in Table 3.14 were used to obtain the ratio for P1 and P2. The values of G (Rel. Pk.) are 0.011 cm^2-sr for P3 and 0.014 cm^2-sr for P4.

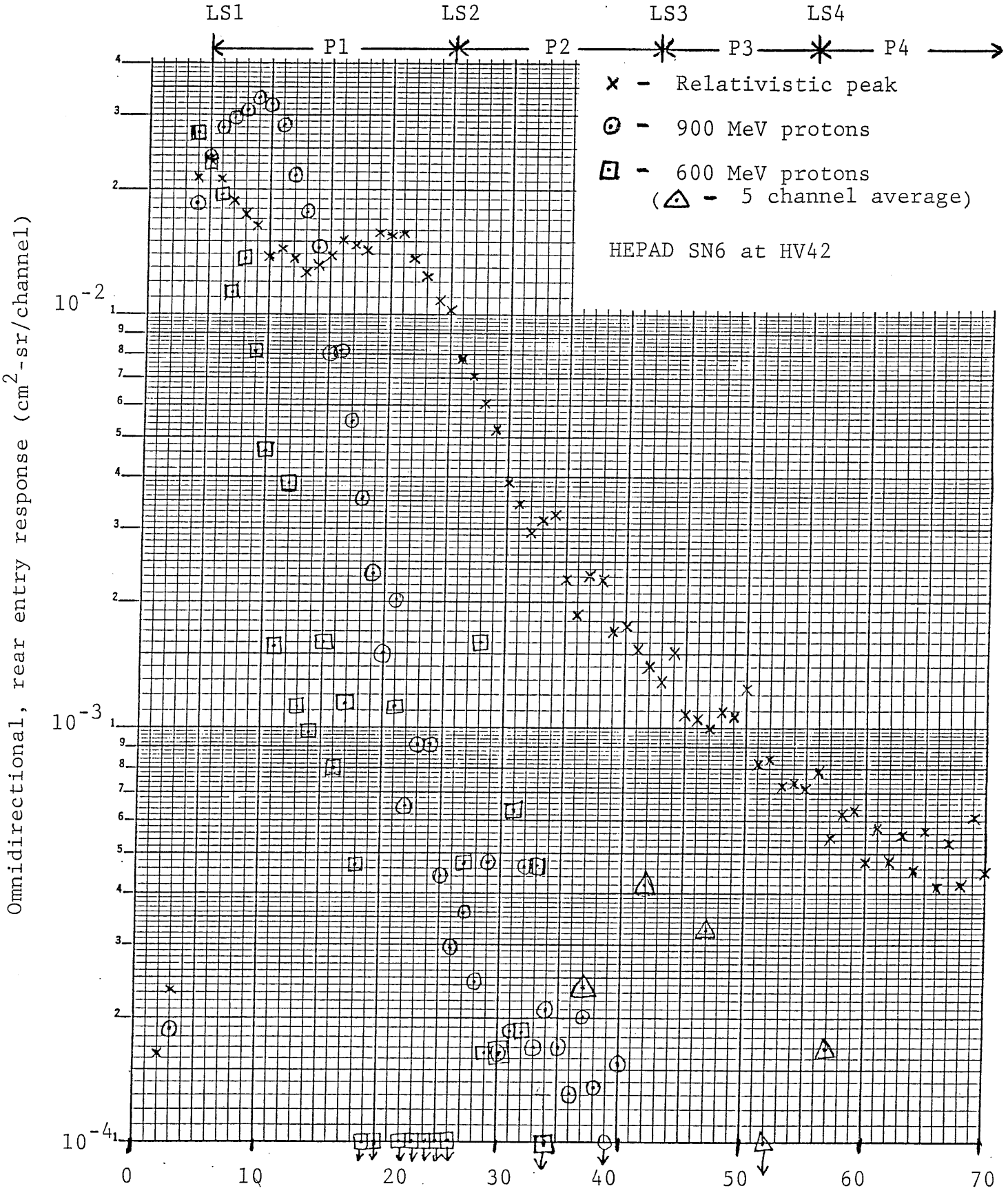

Figure 3.6. HEPAD PMT Spectral Response for Omnidirectional, Rear Entry Particles

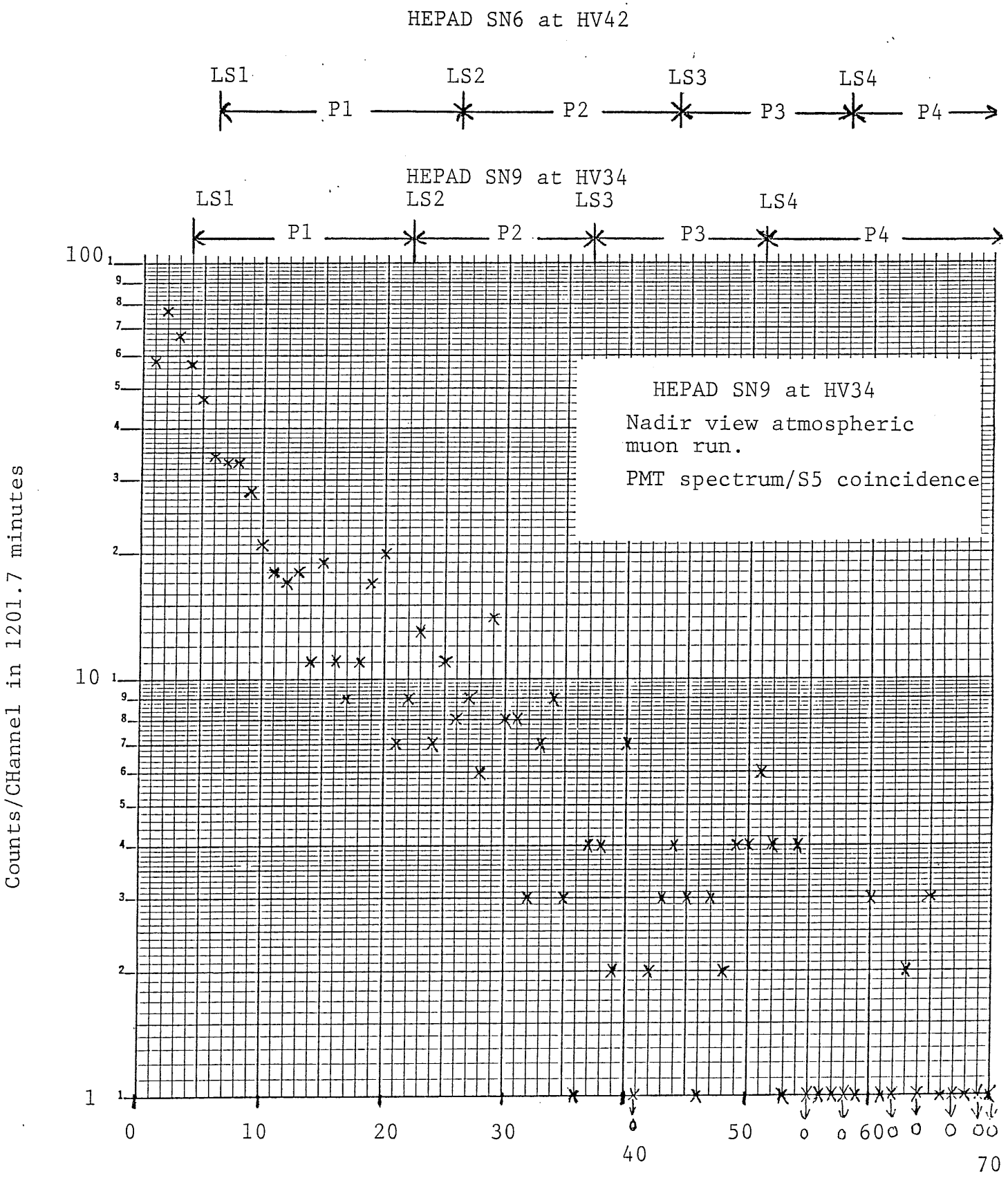

Figure 3.7. HEPAD PMT Spectral Response for Nadir View Atmospheric Muons

Only P1 and P2 need be corrected for rear entry particle response, since the P3 and P4 channel response to high energy front entry particles dominates the small rear entry response (0.74 cm^2-sr vs. about 0.02 cm^2-sr). From the data in Tables 3.14 and 3.15, the P1 channel has a geometric factor of about 0.30 cm^2-sr for protons above about 750 MeV, and the P2 channel has a geometric factor of about 0.08 cm^2-sr for protons above about 1000 MeV. These responses are from rear entry protons, and must be added to the direct front entry responses.

3.5 HEPAD PMT Gain Adjustment and Channel Responses

The HEPAD energy response to protons is determined by the PMT gain, using Fig. 3.5 to obtain the proton energies corresponding to the thresholds LS1 to LS4. For alpha particles the same calibration curve is used with the energies in MeV/nucleon, or about 4X (listed energy); the thresholds (LS5 and LS6) are normalized to the alpha particle relativistic peak, which is 4X (proton relativistic peak). The PMT threshold levels (LS1 to LS6) are fixed in terms of pulse amplitude, and so vary as the PMT gain is changed. From experience it is found that the PMT gain changes with environmental conditions, generally being different in air and vacuum, and that the gain is also expected to decrease with age, use, and radiation exposure.

The PMT gain, and HEPAD energy response, are monitored by the alpha lamp, a plastic scintillator/Am-241 alpha source which produces a stable light pulse output. The alpha lamp is adjusted to give an S4(=LS2)/S3(=LS1) count rate ratio of about 0.5 at the desired PMT gain. This allows monitoring of the HEPAD gain/energy response, and long term adjustment as in-orbit PMT gain changes.

The PMT gain, S3 and S4 count rates, and S4/S3 count rate ratios, were measured vs. PMT HV step, for both HEPADs. The results for SN6 are listed in Table 3.16, where the variation in normalized LS values is also listed. The results for SN9 are listed in Table 3.17. A complication arises because the PMT gain is measured at dynode 10 (DY10), while LS1 to LS6 come from the DY11, DY12, and ANODE signals, as shown in Tables 3.16 and 3.17. A detailed analysis of the PMT dynode voltage distribution and incremental gain changes allows the measured DY10 gain changes to be used to calculate the DY11, DY12, and ANODE gain changes. The measured DY10 gain changes for +1 HV step, and the calculated DY11, DY12, and ANODE gain changes, are listed in Tables 3.16 and 3.17. It is found that a constant factor gain change/HV step is a good description over a wide range of HV step, at least $\pm$ 10 about the nominal operating level. The calculated DY11, DY12, and ANODE gain changes are for a total PMT gain in the range of 10^5 to 10^6, which is the approximate gain of the PMT for normal HEPAD operation.

The normalized LS value changes are opposite to the PMT gain changes because the LS levels are fixed voltage thresholds. The DY11, DY12, and ANODE gain changes are all nearly the same, so an average calculated value has been used for all LS values for each PMT. The slightly different gain factors for SN6 and SN9 are from PMT and HV power supply variations between HEPAD units.

Table 3.16

HEPAD SN6 PMT Gain Adjustment Data

Operating conditions: HV 42 (in air)
S3 = 153 cps; S4 = 10.6 cps; S4/S3 = 0.069
Note: in-orbit cosmic ray background will add about 30 cps to S3 and S4.

HV Step	S3(cps)	S4(cps)	S4/S3	Relative PMT DY10 gain[a]	Relative Normalized LS values[b]
36	150.6	0.44	0.0029	0.785	1.313
38	152.2	1.33	0.0087	0.851	1.199
40	152.0	3.90	0.0257	0.922	1.095
42	152.9	10.61	0.0694	≡1.000	≡1.000
44	155.3	22.5	0.145	1.084	0.913
46	154.6	38.2	0.247	1.175	0.834
48	156.3	59.9	0.383	1.274	0.762
50	157.8	85.2	0.540	1.381	0.696
52	161.4	107.6	0.667	1.497	0.635
54	162.2	126.0	0.777	1.623	0.580
56	165.6	137.7	0.831	1.760	0.530
58	170.6	145.9	0.855	1.908	0.484
60	173.2	147.8	0.853	2.068	0.442

Dynode/Anode	Signal Use	Gain Change for +1 HV Step	
DY10	External Signal Source	x 1.0412	
DY11	LS5 - 6	x 1.0451	Average = x 1.0464
DY12	LS2 - 4	x 1.0475	
ANODE	LS1	x 1.0465	

a) DY10 gain is the change in measured pulse height (alpha lamp, etc.) measured relative to that at HV 42.

b) The LS levels are fixed threshold voltages, so as the PMT gain increases the LS values normalized to the relativistic peak decrease. The gain changes at DY11, DY12, and the ANODE are sufficiently close so that the average gain change has been used for all LS levels.

Table 3.17

HEPAD SN9 PMT Gain Adjustment Data

Operating conditions: HV 34 (in air)
S3 = 187 cps; S4 = 88 cps; S4/S3 = 0.471
Note: in-orbit cosmic ray background will add about 30 cps to S3 and S4.

HV Step	S3(cps)	S4(cps)	S4/S3	Relative PMT DY10 gain[a)]	Relative Normalized LS values[b)]
20	176.1	0.29	0.0016	0.522	2.077
24	177.0	0.43	0.0024	0.628	1.686
26	177.5	0.88	0.0050	0.689	1.518
28	178.0	4.69	0.0263	0.757	1.368
30	179.7	18.1	0.101	0.830	1.232
32	183.4	48.3	0.263	0.911	1.110
33	185.1	68.8	0.371	0.955	1.054
34	187.1	88.1	0.471	≡1.000	≡1.000
35	190.8	110.4	0.579	1.048	0.949
36	195.7	128.4	0.656	1.097	0.901
38	204.4	153.2	0.750	1.204	0.812
40	222.5	168.0	0.755	1.322	0.731
42	243.1	173.5	0.714	1.451	0.659
44	270.7	174.7	0.645	1.592	0.593
46	307.4	177.2	0.576	1.747	0.534
50	408.0	180.3	0.442	2.104	0.434

Dynode/Anode	Signal Use	Gain Change for +1 HV Step	
DY10	External Signal Source	x 1.0476	
DY11	LS5 - 6	x 1.0522	Average = x 1.0536
DY12	LS2 - 4	x 1.0549	
ANODE	LS1	x 1.0537	

a) See Footnote in Table 3.16.

b) See footnote in Table 3.16.

The actual in-orbit HEPAD particle energy levels for P1 to P4 and A1, A2 are obtained from the measured S4/S3 count rate ratio, using Tables 3.16 and 3.17 to obtain the LS level correction factor, and then using the corrected LS levels in Fig. 3.5 to obtain the energy ranges for each channel. Note that the in-orbit S3 and S4 count rates will have a high energy, cosmic ray proton background added on, and this must be used to correct the ground-based S3/S4 data listed in Tables 3.16 and 3.17 (see Refs. 4 and 6 for in-orbit data for the GOES-D, -E and -F HEPADs). Note also that PMT gain adjustment/measurement can only be made during low ambient particle flux periods, since the presence of high energy solar protons will change the S3 and S4 count rates significantly, while high energy electron bremsstrahlung can also affect the S3 count rate through Cerenkov light from Compton scattered electrons in the PMT quartz radiator.

The in-orbit PMT gain measurement data obtained from Tables 3.16 and 3.17 (the relative normalized LS value factors are needed) are then used with the baseline normalized LS values to obtain the HEPAD particle energy response. The baseline LS values, normalized to the 12° relativistic peak, are given in Tables 3.18 for SN6 and 3.19 for SN9. These are the values from Table 3.10 for LS1 to LS4, while LS5 and LS6 are obtained as described in the Tables. For LS5 and LS6 the levels are also listed as 4X (value), where (value) can now be used directly in Fig. 3.5 to obtain the alpha particle energies in MeV/nucleon.

Tables 3.18 and 3.19 also give the Fig. 3.5 calibration curve proton energies for LS1 to LS4, and alpha particle energies for LS5 and LS6. The $\pm$ 1σ ΔEp values give the approximate energy range over which the channel response goes from 16% to 84% of full response (for turn-on), and are obtained from the $\pm$ 1σ curves in Fig. 3.5. The $\pm$ 1σ ΔEp values are in good agreement with the detailed channel responses in Figs. 3.3 and 3.4, although for E_p > 600 MeV the response becomes asymmetric (e.g., P3 has a long, high-energy tail - see Figs. 3.3 and 3.4).

The final column in Tables 3.18 and 3.19 gives the level responses for a + 1HV step gain change in the HEPAD PMTs. The relative normalized LS value factors of Tables 3.16 and 3.17 (0.956 for SN6 and 0.949 for SN9) were used to multiply the LS level values in Tables 3.18 and 3.19, and these corrected LS values were then used in Fig. 3.5 to obtain the new E_p values. Note that the approximate 5% gain increase (level <u>decrease</u> of about 5%) results in only small shifts for LS1 to LS3, and LS5, while the highest levels LS4 and LS6 allow the largest changes. The values for P1 to P4 and A1, A2 are obtained from the LS energy thresholds since

P1	=	LS1 to LS2
P2	=	LS2 to LS3
P3	=	LS3 to LS4
P4	=	LS4 to LS5
A1	=	LS5 to LS6
A2	=	> LS6

Table 3.18

HEPAD SN6 Detected Particle Energies

Values as for operation at HV42 (in air), with
S3 = 153 cps, S4 = 10.6 cps, S4/S3 = 0.069

Level Designation	Level 12° rel. pk.	Calib. Curve (Fig. 3.5) E_p (MeV)	Approximate $\pm$ 1 σ ΔE_p (MeV)	For +1 HV Step E_p (MeV)
LS1	0.074	355	$\pm$ 15	353
LS2	0.346	435	$\pm$ 25	430
LS3	0.579	555	$\pm$ 60	540
LS4	0.765	760	$\pm$ 150	705
LS5 (alphas)	2.63 (4x0.66)	4 x 625	$\pm$ (4x90)	4x595
LS6 (alphas)	3.09 (4x0.77)	4 x 770	$\pm$ (4x150)	4x720

Note: LS1 to LS4 are taken from Table 3.10. LS5 and LS6 were obtained from the HEPAD IFC measured values, normalized to LS4. These values are in good agreement with the nominal theoretical values used for the earlier HEPADs.

Table 3.19

HEPAD SN9 Detected Particle Energies

Values are for operation at HV 34 (in air), with
S3 = 187 cps, S4 = 88 cps, S4/S3 = 0.471

Level Designation	Level 12° rel. pk.	Calib. Curve (Fig. 3.5) E_p (MeV)	Approximate $\pm$ 1 σ ΔE_p (MeV)	For +1 HV Step E_p (MeV)
LS1	0.061	350	$\pm$ 15	350
LS2	0.338	430	$\pm$ 25	425
LS3	0.566	545	$\pm$ 55	530
LS4	0.780	780	$\pm$ 150	720
LS5 (alphas)	2.83(4x0.71)	4 x 675	$\pm$ (4x130)	4 x 640
LS6 (alphas)	3.33(4x0.83)	4 x 925	$\pm$ (4x250)	4 x 810

Note: LS1 to LS4 are taken from Table 3.10. LS5 and LS6 are from Table 3.5, divided by 0.928 as was done for LS1 to LS4 in Table 3.10.

The HEPAD geometric factors can be taken as flat at the peak value over the appropriate LS energy range, and zero outside that energy range. For most cases this is a good enough approximation to give reasonably accurate fluxes. Note however that P1 and P2 must in some cases have the high energy response from rear entry particles subtracted. Note that the peak geometric factors in some channels do not reach the full HEPAD value (Figs. 3.3 and 3.4). This is because three channels all have some response to a given proton energy. The integral of channel geometric factor over all response energies will, however, be the same as the total HEPAD geometric factor times the channel energy range (energies from Fig. 3.5, as listed in Tables 3.18 and 3.19). In some cases it may be desirable to use the more detailed channel response curves shown in Figs. 3.3 and 3.4, adjusted, if necessary, for slight PMT gain difference. In general, however, the sharp-edged (box) response approximation should be adequate.

4.0 SUMMARY AND CONCLUSIONS

Two HEPADs, SN6 and SN9, have been calibrated with proton beams at the BNL AGS. The beam-defining apparatus succeeded in eliminating spurious peaks, and HEPAD calibration data were obtained for narrow energy range proton beams. Angular response data for front and rear entry protons were obtained and compared with atmospheric muon responses. A detailed calibration at 12° was performed.

The front entry angular response data show that the 12° response gives a good approximation to the omnidirectional response, accurate to $\pm 5\%$. The atmospheric muon zenith view response is equal to the 12° relativistic particle response also to $\pm 5\%$. A detailed calibration curve for protons at 12° was obtained, with good agreement between the P1 to P4 channel response data and the PMT spectra data. Results for both HEPADs and earlier calibrations in Ref. 2 are all in good agreement. The final calibration curve (Fig. 3.5) differs somewhat from an earlier BNL AGS data-derived calibration curve (Refs. 3,4) because the earlier data were contaminated by higher energy protons.

The lowest energy channels, P1 and P2, have some contamination by high energy rear entry particles. The rear entry BNL AGS data for the relativistic peak are in good agreement with nadir view atmospheric muon runs. The measured response curves (Fig. 3.6) can be used to estimate the rear entry response for HEPADs with different level sensor (LS) values for P1 and P2.

The final PMT gain adjustment data for the alpha lamp outputs in SN6 and SN9 are given in tabular form, and allow in-orbit gain adjustment and measurement. The gain-corrected LS values can then be calculated and the channel responses for P1 to P4 and A1, A2 can be obtained from Fig. 3.5. The response widths (rise and fall of each channel) can be estimated from $\pm 1\sigma$ curves provided with the final calibration curve in Fig. 3.5.

The HEPAD can now be considered a fully calibrated instrument, with its proton and alpha particle response well understood. Atmospheric muon runs, zenith and nadir view, can be used to provide absolute gain calibration for the HEPAD. Any HEPAD using the identical detector geometry and shielding configuration and the same electronic pulse processing should have the same response as given in this report.

REFERENCES

1. Proton Calibration Plan for HEPAD at the Alternating Gradient Synchrotron of Brookhaven National Laboratory, Panametrics, Inc., PANA-NOAA-TP2 (March 25, 1986).

2. M.C. Rinehart, Cerenkov Counter for Spacecraft Application, Nucl. Inst. and Meth. 154, 303-316 (1978).

3. March, 1980 HEPAD Tests, SN6 and SN8, Preliminary Data Analysis, Panametrics, Inc., PANA-SEM-1 (July 18, 1980).

4. GOES-D, -E, and -F HEPAD's, Report on Ground-Based Tests and on In-Orbit Operations for GOES-D and -E, Panametrics, Inc., PANA-SEM-5 (May 2, 1983).

5. J.F. Janni, Calculations of Energy Loss, Range, Pathlength, Straggling, Multiple Scattering, and the Probability of Inelastic Nuclear Collisions for 0.1 to 1000-MeV Protons, Tech. Rep. No. AFWL-TR-65-150, AFWL/AFSC, Kirtland AFB, New Mexico (Sept. 1966).

6. Determination of the Operating HV Step of the HEPAD S/N 3 In-Orbit on the GOES-F (-6) Satellite, Panametrics, Inc., PANA-SEM-6 (August 16, 1983).